UCRL-50174 Rev. 1

INTERNATIONAL TABLES

FOR

X-RAY CRYSTALLOGRAPHY

VOL. IV

CIRCULATION COPY
SUBJECT TO RECALL
IN TWO WEEKS

SECTION 2.1

LOAN
COPY

DISCLAIMER

This document was prepared as an account of work sponsored by an agency of the United States Government. Neither the United States Government nor the University of California nor any of their employees, makes any warranty, express or implied, or assumes any legal liability or responsibility for the accuracy, completeness, or usefulness of any information, apparatus, product, or process disclosed, or represents that its use would not infringe privately owned rights. Reference herein to any specific commercial product, process, or service by trade name, trademark, manufacturer, or otherwise, does not necessarily constitute or imply its endorsement, recommendation, or favoring by the United States Government or the University of California. The views and opinions of authors expressed herein do not necessarily state or reflect those of the United States Government or the University of California, and shall not be used for advertising or product endorsement purposes.

This report has been reproduced
directly from the best available copy.

Available to DOE and DOE contractors from the
Office of Scientific and Technical Information
P.O. Box 62, Oak Ridge, TN 37831
Prices available from (615) 576-8401, FTS 626-8401

Available to the public from the
National Technical Information Service
U.S. Department of Commerce
5285 Port Royal Rd.,
Springfield, VA 22161

Work performed under the auspices of the U.S. Department of Energy by Lawrence Livermore National Laboratory under Contract W-7405-ENG-48.

2.1. X-ray Cross Sections and Attenuation Coefficients

2.1.1. Introduction

Uncertainties in the values of absorption corrections represent perhaps one of the most serious systematic errors in the derivation of structure factors from Bragg intensity data. Critical to these corrections are reliable values of the attenuation coefficients† for the elements. Recent experimental and theoretical work has produced values for these coefficients which are considerably more reliable than those that appear in Volume III, Tables 3.3.2. Tabulations of X-ray cross sections σ in 10^{-24} cm²/atom (barns/atom) are given in Table 2.1B, and attenuation coefficients (μ/ρ) in cm² g^{-1} are given in Table 2.1C for the wavelengths commonly used in crystallography. These wavelengths and energies are identified in Table 2.1A. Users who wish to compare these values with those in Volume III should note carefully that although the values in Table 2.1C may be directly compared with those in Table 3.2.2A of Volume III, the cross sections σ (called μ in Volume III) have units of 10^{-23} cm² in Table 3.2.2B of Volume III but 10^{-24} cm² in Table 2.1B of this volume. Users should also read carefully Section 2.1.4 regarding the reliability of these values.

The linear absorption coefficient μ may be obtained in two ways. From the attenuation coefficients (mass absorption coefficients), we have

$$\mu=\rho\sum_i g_i(\mu/\rho)_i \qquad \ldots.(1)$$

where g_i is the mass fraction of element i, with attenuation coefficient $(\mu/\rho)_i$, and ρ is the density of the material. The summation is over all constituent elements. For a crystal with unit-cell volume V_c, we may obtain μ from the cross sections,

$$\mu=\frac{1}{V_c}\sum\sigma_i \qquad \ldots.(2)$$

The summation is over all atoms in the cell. (Note that if σ_i is in barns/atom and V_c is in Å^3, μ is in cm^{-1}.)

The values in Tables 2.1B and 2.1C are interpolated from an evaluated cross-section compilation by McMaster *et al.* [33] over the photon energy range 1 keV to 1 MeV (12·4 to 0·124 Å).

That compilation was constructed by subtracting theoretical scattering cross sections from measured total cross sections (attenuation coefficients). The differences obtained from this subtraction process were, for the purpose of this compilation, assumed to be photoeffect‡ cross sections. In addition to photoeffect cross sections (a) inferred from measured total attenuation coefficients, two other types of photoeffect data were included in the analysis: (b) explicitly measured photoeffect cross sections and (c) available numerical theoretical estimates of the photoeffect. Fitting and interpolation procedures were then applied to a combination of these three types of photoeffect data. In the fitting procedures, weights ranging from 1 to 10, based on an evaluation by McMaster *et al.* of each experiment or calculation, were assigned to the various data sources. This weighting procedure allowed the use of a broad base of input data and at the same time maximized the impact of available high-accuracy data on the compilation.

2.1.2. Sources of Information

The input information to the compilation of reference [33], from which this compilation is derived, includes principally the following.

2.1.2.1. Experimental Attenuation Coefficient Data

Experimental total attenuation coefficient data for 69 elements were extracted in numerical form from 71 published and unpublished sources listed in References [52]–[123]. These sources were judged by McMaster *et al.* [33] to contain data of adequate accuracy to be useful as input to the compilation. Some of the points considered as bases for rejection of data in this evaluation include:

(1) Inadequate correction for sample impurities,
(2) Poor collimation resulting in unwanted detection of small-angle scattering,
(3) X-ray source insufficiently mono-energetic,
(4) Obvious typographical errors, and
(5) Unexplainable systematic errors.

This compilation ignores Kossel-type, Kronig-type, or other fine structure§ in the photoeffect near absorption

†Although the name *absorption coefficient* has had wide use in the literature in referring to the total photon interaction cross section in macroscopic units, we here follow the present nomenclature of the International Commission on Radiation Units and Measurements contained in ICRU Report 11 [26] (see also [12], [19], [49]) in using the name *attenuation coefficient* for this quantity. This nomenclature allows a clear distinction from the *absorption coefficient* used in X-ray dosimetry (see, for example, [2], [5], [48], [17]) to denote the product of the attenuation coefficient and the average fraction of incident photon energy not lost from the interaction site in the form of scattered secondary photons.

‡"Photoeffect" and "photoelectric effect" are used interchangeably in this article.

§ See, *e.g.*, the early studies of edge structure by Stenström [46], Kossel [28], and Kronig [29], and the later reviews of experimental and theoretical information by Cauchois [7], Faessler [18], Sandström [43], Parratt [37], and Azároff [3].

The structure very close to an absorption edge (less than ~30 eV above the edge) is generally referred to as "Kossel structure". Peaks and trenches in this region, which can differ by a factor of two or more from the smoothly extrapolated values in this compilation, can occur even for isolated atoms, as has been shown, for example, for Ar gas by Parratt [36]. Kossel structure can be described in terms of transitions of the (very-low-energy) ejected electron to unfilled discrete energy states of the atom (or molecule), rather than to the continuum of states beyond a characteristic energy. Superimposed on the close-in Kossel structure is the so-called "Kronig structure" which persists a few hundred eV above the absorption edge (usually to ~200 or 300 eV but occasionally to nearly 1 keV above an edge [31], [13]) (see [151] added in proof). This more extended Kronig

edges, but rather extrapolates smoothly back to an idealized "single sawtooth" for each edge. Hence, some high-resolution data of otherwise adequate accuracy were omitted from the input. For example, in the detailed L-edge studies by Nordfors and Noreland [104], and Ekstig [82], only the data points furthest from the edges were used for this compilation.

2.1.2.2. Experimental Photoeffect Data

The explicit total photoeffect cross sections measured by Titus [50] and by Parthasaradhi *et al.* [38] were included as input to the compilation.

2.1.2.3. Theoretical Photoeffect Data

The numerical theoretical values of Schmickley and Pratt [44], which combine their own results with those of Rakavy and Ron [41] and Hultberg, Nagel, and Olsson [24], were used, and also the values calculated by Brysk and Zerby [6]. The Schmickley–Pratt results include screening and relativistic effects in a central-field approximation and provide K through M_V subshell cross sections of Fe, Sn, and U for 412 to 1332 keV photon energies. Similar results by Rakavy and Ron [24] provide K through O_V subshell cross sections of Al, Fe, Sn, W, and U for 1 to 2000 keV photon energies. The unscreened Coulomb-field results of Hultberg, Nagel, and Olsson provide K-shell cross sections only for H, Be, C, N, O, Al, Cu, Zn, Se, Mo, Ag, Sn, Ta, Pt, Au, Pb, Po, Th, U, Cm, and Fm for photon energies 1 keV to 10 MeV. Schmickley and Pratt were able to use the latter data by noting that the ratio of screened to unscreened photoeffect cross section for a given subshell is, to a good approximation, equal to the square of the renormalization factor in going from the unscreened to a screened bound-state wave function. These renormalization factors were computed using the results of Liberman, Waber, and Cromer [30] based on the relativistic Hartree–Fock–Slater potential. Schmickley and Pratt also included the theoretical results of Pratt *et al.* [40], Alling and Johnson [1], and Hall and Sullivan [21] in their analysis.

2.1.2.4. Theoretical Coherent Scattering Data

Coherent (Rayleigh) scattering cross sections were evaluated using the relativistic Dirac–Slater atomic scattering factors calculated by Cromer and Waber [10].

2.1.2.5. Theoretical Incoherent Scattering Data

Incoherent (Compton) scattering cross sections were evaluated using the relativistic Dirac–Slater (with exchange) incoherent scattering factors calculated by Cromer and Mann [9] and Cromer [8].

2.1.3. Compilation Procedure

2.1.3.1. Synthesis of Photoeffect Cross Sections from the Experimental and Theoretical Input Information

The mass attenuation coefficient, μ/ρ, is related to the total photon-atom interaction cross section, σ_{tot}, according to

$$\frac{\mu}{\rho}(\mathrm{cm^2/g}) = (N_A/M)\cdot\sigma_{tot}(\mathrm{cm^2/atom}) \qquad \ldots(1)$$
$$= (N_A/M)\cdot 10^{-24}\cdot\sigma_{tot}(\mathrm{barns/atom})$$

where

N_A = Avogadro's number = $6{\cdot}02252\times10^{23}$ atoms/gram atom

and, for this value of N_A,

M = atomic weight relative to $M(^{12}\mathrm{C}) = 12{\cdot}0000$.

The "barn":

1 barn = 10^{-24} cm^2

is a convenient unit for expressing values of the atomic cross sections.

The total atomic cross section, σ_{tot}, in turn, can be represented in this energy range by the sum

$$\sigma_{tot} = \tau + \sigma_{coh} + \sigma_{incoh} \qquad \ldots(2)$$

in which the photoeffect cross section, τ, the coherent scattering cross section, σ_{coh}, and the incoherent scattering cross section, σ_{incoh}, depend in different ways on the atomic number, Z, and the photon energy, E (or wavelength, λ). For purposes of constructing this compilation, the scattering cross sections σ_{coh} and σ_{incoh} were considered "known"† and calculable according to (see, for example, [19], [16], [12], [51], [23]):

$$\sigma_{coh} = \frac{1}{2}r_0^2\int_{-1}^{1}(1+\cos^2\phi)\cdot f^2(x,Z)\cdot 2\pi\, d(\cos\phi) \qquad \ldots(3)$$

and

$$\sigma_{incoh} = \frac{1}{2}r_0^2\int_{-1}^{1}\left\{[1+k\,(1-\cos\phi)]^{-2} \times\left[1+\cos^2\phi+\frac{k^2(1-\cos\phi)^2}{1+k(1-\cos\phi)}\right]\right\} \times Z\cdot S(x,Z)\cdot 2\pi\, d(\cos\phi) \qquad \ldots(4)$$

structure can be described in terms of interference effects on the de Broglie wave of the ejected electron by the molecular (see, *e.g.*, Hartree, Kronig, and Peterson [22]) or crystalline spatial ordering of neighboring atoms. Kronig structure oscillations of the order of 50% sometimes persist as far as 50–60 eV above an absorption edge [14]. However, based on the literature examined, this structure in the region beyond ~200 eV above an edge is usually [18] confined to an envelope of the order of 15% above and below the smoothly extrapolated compiled cross-section values (see [151] added in proof). Both the Kossel- and the Kronig-type fine structures can vary widely in magnitude and in energy displacement of the features, depending on the molecular, crystalline, or thermal environment of the atom, as has been recently discussed by Deslattes [14].

† For photon energies above 100 keV there is experimental evidence [35], [15] suggesting that present incoherent scattering theory for whole atoms, which neglects the effects of initial electron velocities, underestimates scattering into backward directions, and, in turn, the total incoherent scattering cross section. However, in the energy range considered here we assume that this process is adequately described by present theory.

in which

$r_0^2 = 7{\cdot}9398 \times 10^{-26}$ cm^2, the square of the classical electron radius,

ϕ = the angle between the incident and scattered photon directions $= 2\theta$ where θ is the Bragg-angle parameter used, *e.g.* by Ibers [25], Curien [11], and Cromer [8],

$2\pi\, d(\cos\phi) = d\Omega$ = the solid angle between cones with angles ϕ and $\phi + d\phi$,

k = incident photon energy in mc^2 units $= E(\text{keV})/511{\cdot}006 = [12{\cdot}398/\lambda(\text{Å})]/511{\cdot}006$,

Z = atomic number,

$f(x, Z)$ = atomic scattering factor given by Cromer and Waber [10] as a nine-parameter analytical fit to their theoretical data,

$S(x, Z)$ = incoherent scattering factor tabulated by Cromer and Mann [9] and Cromer [8], and

$x = \left(\sin\frac{\phi}{2}\right)/\lambda(\text{Å}) = (\sin\theta)/\lambda(\text{Å})$ = momentum transfer parameter.

For hydrogen the analytic expressions from Pirenne [39] were used:

$$f(x, 1) = (1 + 4\pi^2 a_0^2 x^2)^{-2} \qquad \ldots.(5)$$

and

$$S(x, 1) = 1 - [f(x, 1)]^2 \qquad \ldots.(6)$$

where

a_0 = the first Bohr radius = 0·529167 Å

The remaining term on the right side of equation (2), the photoeffect cross section, τ, was evaluated from available experimental and theoretical information for approximately 10,000 combinations of Z and E covering 87 elements and the energy range 1 keV to 1 MeV. The following paragraphs describe the methods by which these 10,000 values of τ were obtained.

(1) Measured mass attenuation coefficient data (of acceptable accuracy) were utilized throughout the region in which the sum of the scattering cross sections, $\sigma_{\text{coh}} + \sigma_{\text{incoh}}$ comprises less than 95% of the total cross section, σ_{tot}. From these measured data, values of the photoeffect cross section were evaluated according to

$$\tau = \sigma_{\text{tot}} - (\sigma_{\text{coh}} + \sigma_{\text{incoh}}) \qquad \ldots.(7)$$

(2) The measured explicit photoeffect data of Titus [50] for Cu, Mo, Ag, Ta, and Au at 662 keV and of Parthasaradhi *et al.* [38] for Cu, Ag, Sn, Ta, Pt, and Pb at 145, 320, and 662 keV were used directly.

(3) The theoretical photoeffect data of Schmickley and Pratt [44] for energies above 10 keV were used for elements with $Z = 13$, 20, 26, 29, 42, 47, 50, 60, 74, 78, 79, 82, 84, and 92. Also included in the theoretical photoeffect data were the results of Brysk and Zerby [6], Rakavy and Ron [41], and for hydrogen the results of Samson [42] and Seltzer [45].

(4) A third-order log-log least-squares fit to the above theoretical values of τ was made across Z to obtain interpolated theoretical values of τ for the remaining compilation elements.

(5) Two types of further third-order log-log least-squares fits were made: (a) using all elements in the compilation and (b) using only those elements for which the best experimental data (uncertainties less than 2%) exist.

2.1.3.2. Photoeffect Data Fitting

The values of the photoeffect cross section, τ, obtained as above were, for each of the 87 compilation elements, fitted by least squares to a log-log polynomial in incident photon energy between each absorption-edge region:

$$\ln \tau_j = \sum_{i=0}^{1,2 \text{ or } 3} a_{ij} \{\ln[E(\text{keV})]\}^i \qquad \ldots.(1)$$

In this polynomial, the total photoeffect cross section τ_j represents one of the sums:

$$\tau_1 = \tau_K + \tau_L + \tau_M + \tau_N + \ldots$$
$$\tau_2 = \tau_L + \tau_M + \tau_N + \ldots$$
$$\tau_3 = \tau_M + \tau_N + \ldots$$
$$\tau_4 = \tau_N + \ldots$$

over contributions from the K shell, L shell, or higher shells of the atom where applicable.

It was in making the fit in equation (1) that the values of τ were weighted from 1 to 10 depending on claimed experimental accuracy or the accuracy as evaluated by McMaster *et al.* Theoretical and interpolated τ-data were all weighted 1. In Section III of Reference [33] McMaster *et al.* list all these datapoints, their assigned weights, and the total (compilation) cross sections, reconstructed using equation 2.1.3.1(2), in the form of per cent differences from the listed source-identified input values of μ/ρ.

The fitted coefficients a_{ij} for the log-log representation in equation (1) are given in Section II of Reference [33]. These may be used for generating cross sections consistent with this compilation at additional wavelengths or photon energies.

No fits were made within multiple-edge regions (*e.g.* between the L_{I} and L_{III} edge-energies or between the M_{I} and M_{V} edge-energies) indicated in Fig. 2.1.3.2. The cross sections in these regions were obtained by using "jump ratios" (τ just above an absorption edge divided by τ just below that absorption edge) calculated from the theoretical individual subshell data of Rakavy and Ron [41]. The fit in equation (1) to the energy region just above each edge-group was successively divided by the appropriate jump ratio to extend the compilation down in energy through the edge-group region. The edge-region cross sections thus obtained for the compilation were checked graphically

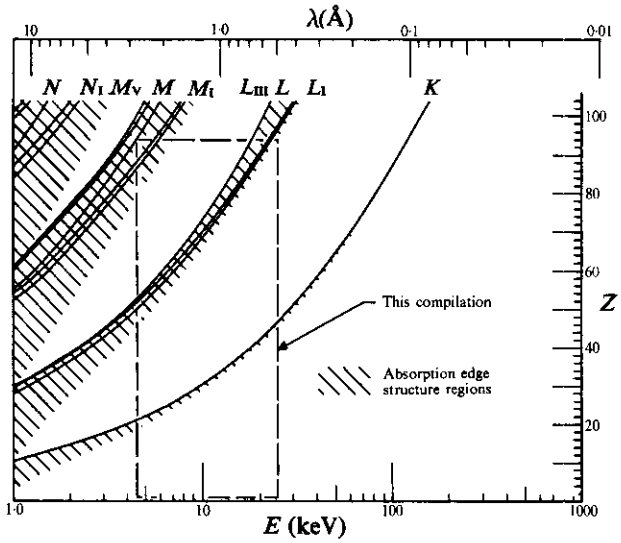

Fig. 2.1.3.2. Regions (indicated by hash marks) of Tables 2.1B and 2.1C likely to have $>5\%$ uncertainties because of photoeffect absorption-edge fine structure. The edge-values are taken from Hagström *et al.* [20] and Bearden and Burr [4].

and found to lie within the spread of available experimental data-points. The edge energies used are those of Hagström *et al.* [20].

2.1.4. Uncertainty of the Compilation Values

The authors have estimated the ranges of uncertainties in values of the total photon interaction cross section σ_{tot} (or mass attenuation coefficient, μ/ρ), in Reference [33] and in Tables 2.1B and 2.1C. These ranges of uncertainties fall into four categories:

A: $\pm<2\%$
B: ± 2–5%
C: ± 5–15% and
D: $\pm>15\%$

Category A ($\pm<2\%$): This category applies (except near absorption edges as noted in Categories C and D, below) over the energy region 6 to 40 keV for the following elements: C, Mg, Al, Ti, Fe, Ni, Cu, Zn, Zr, Mo, Pd, Ag, Cd, Sn, La, Gd, Ta, W, Pt, Au, Pb, Th, and U. For these elements in this energy range, in the authors' opinion, there are an adequate number of independent experimental data-sources, with sufficient overlap and consistency to assign a $\pm 2\%$ envelope of uncertainty.

The authors also include in Category A the region above 100 keV for all elements where incoherent scattering comprises more than 90% of the total cross section.

Category B (± 2–5%): Except for the low-Z elements singled out for Category C, below, Category B applies to the energy region 2–6 keV for all elements, 6–40 keV for elements not specified in Category A, above, and above 40 keV except for the scattering-dominated region specified in Category A, above. For energies above 2 keV, it was noted that available experimental data could be represented by least-squares third-order log-log fits across Z. The degree of consistency of the individual data-points for well-measured elements with these fits formed a partial basis for the $\pm 5\%$ uncertainty assigned to Category B data, since the compilation relies on such fits in interpolating data from well measured elements to intermediate poorly measured elements.

Category C (± 5–15%): The authors include in Category C:

(1) the elements hydrogen, helium, and lithium,
(2) the energy region 1–2 keV for all elements, and
(3) the regions containing K, L, M, and N absorption edges, and the fine-structure regions extending 1 keV above each of these regions, as indicated in Fig. 2.1.3.2. An exception is the ($\pm>15\%$) region extending ~ 200 eV just above each edge which the authors place in Category D, below.

In (1) and (2), above, the experimental uncertainties or inconsistencies in some cases greatly exceed 15%. However, the total cross section in these regions is considered known theoretically, except for the edge-structure regions, to within this uncertainty.

Category D ($\pm>15\%$): Kossel- and Kronig-type fine structure within ~ 200 eV of an absorption edge, as has been discussed in Section 2.1.2 (footnote), can exhibit peaks and(or) trenches which can vary by a factor of two or more from the smoothly extrapolated values in this compilation. Examples of such features, and their comparison with this compilation, are shown in Figs. 2.1.4(1)–(2) (from [84], [151]). These features, both in magnitude and energy displacement, depend critically on the molecular, chemical, crystalline, thermal, or other environment of the atom.

Figs. 2.1.4(3)–(6) show a comparison of the present compilation and another recent extensive compilation (Storm and Israel [48]) with available experimental data and with theoretical photoeffect data in the region where $\sigma_{tot}\sim\tau_{tot}$. These comparisons contain examples of Category A, B, and C data as described above, and may be helpful in allowing an independent judgment by the reader of the uncertainties in values of σ_{tot} and μ/ρ in Tables 2.1B and 2.1C.

The σ_{tot} values in Figs. 2.1.4(3)–(6) above 1000 keV are taken from NSRDS-NBS Report 29 [23]. These values are not significantly different from those given in the LASL report by Storm and Israel [48].

Acknowledgment

The authors thank J. W. Cooper and R. D. Deslattès for helpful comments and suggestions on this material.

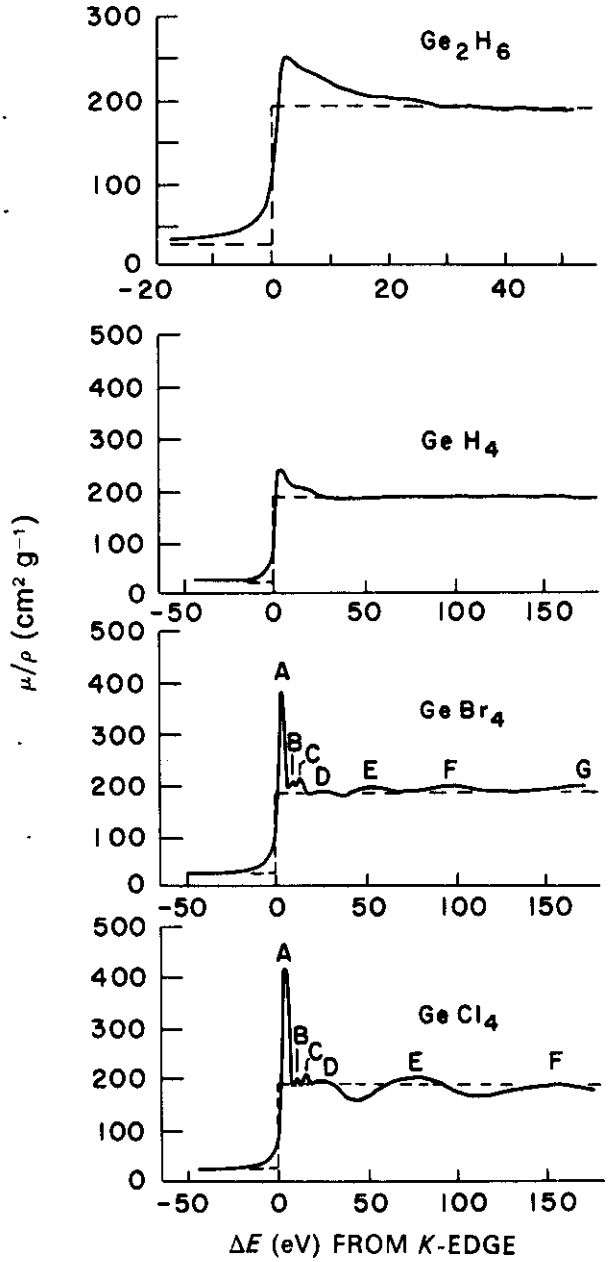

Fig. 2.1.4(1). Values of μ/ρ for germanium, measured with a double-crystal diffraction spectrometer, in Ge_2H_6 (digermane), GeH_4 (germane), $GeBr_4$ (germanium tetrabromide), and $GeCl_4$ (germanium tetrachloride) in the vicinity of the Ge K-edge (11·104 keV) (Glaser [84]). The dashed lines are Ge μ/ρ values taken from reference [33] from which Tables 2.1B and 2.1C are derived.

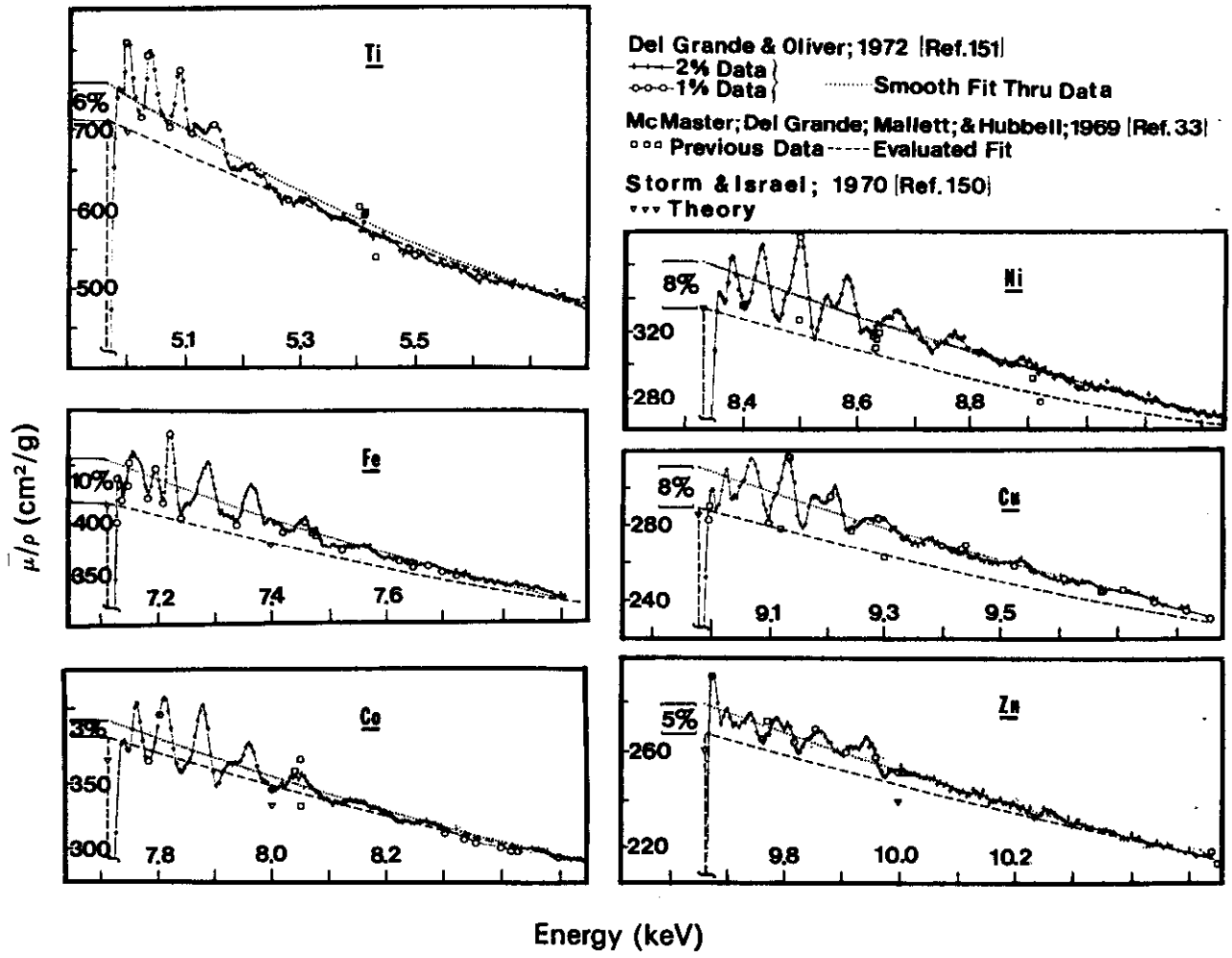

Fig. 2.1.4(2). Recent total attenuation-coefficient measurements for the energy region extending almost 1 keV above the respective K-absorption edges of titanium, iron, cobalt, nickel, copper, and zinc by Del Grande and Oliver [151] are shown together with previous measurements evaluated by McMaster *et al.* [33]. The discrepancies are within the uncertainties discussed in Section 2.1.4 (*i.e.* see Categories C and D). Also included for purposes of comparison are the Storm and Israel values [150] based predominantly on relativistic Hartree–Fock–Slater calculations.

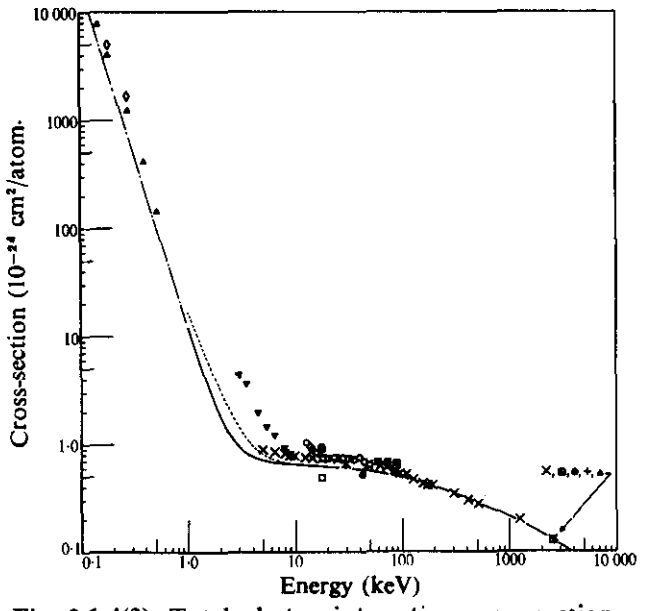

Fig. 2.1.4(3). Total photon interaction cross section, σ_{tot}, for hydrogen. The theoretical photoeffect cross section (—·—·—) calculated independently by Samson [42], Schmickley [149], and also by Seltzer [45], extends above 1 keV, and was the primary source of photoeffect data for this element in constructing the compilation of reference [33] shown by the solid line. The Storm and Israel [48] compilation (-----), where significantly different, is shown for comparison [150]. The experimental values are from [88], [132], [56], [131], [106], [126], [113], [144], [146], [137], [65], and [128].

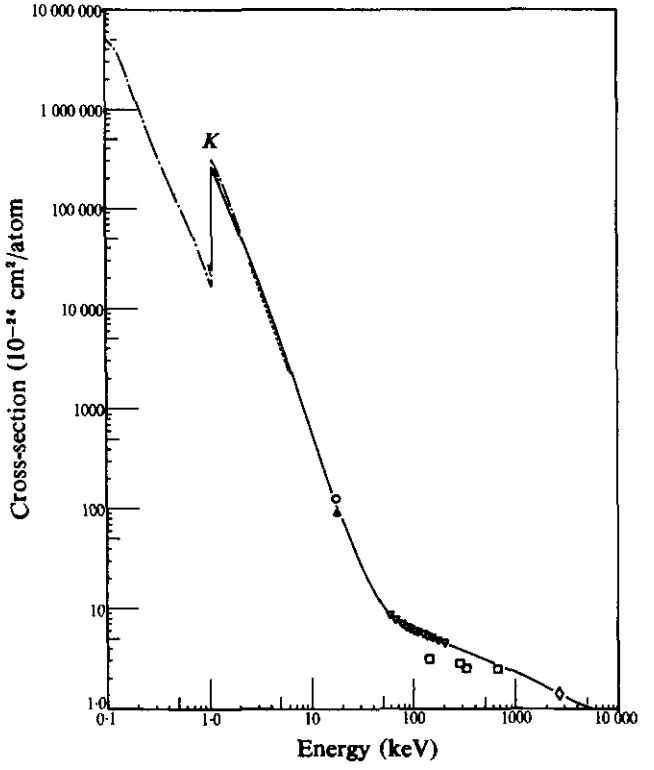

Fig. 2.1.4(4). Total photon interaction cross section, σ_{tot}, for sodium. The McGuire [32] theoretical photoeffect results (—·—·—) and the Storm and Israel [150] values (.....) not included in the analysis of reference [33], are shown for comparison here and in Figs. 2.1.4(5)–(6). The experimental values are from [127], [113], [73], [109], [128].

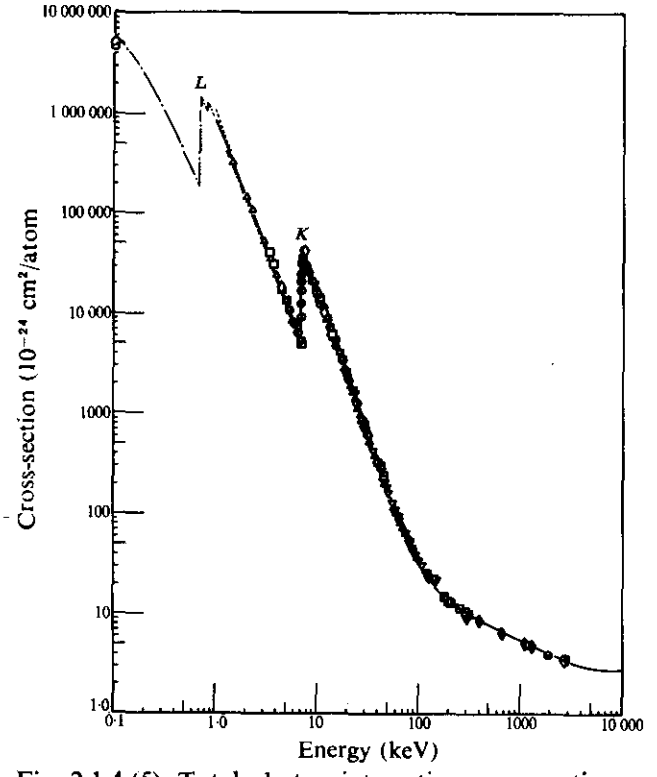

Fig. 2.1.4.(5). Total photon interaction cross section, σ_{tot}, for iron. In using the theoretical photoeffect data of Rakavy and Ron [41] contributions from missing subshells were estimated and applied, a correction not negligible at the lowest energies. The experimental values are from [143], [63], [74], [81], [77], [69], [99], [79], [125], [127], [121], [124], [148], [141], [95], [118], [136], [111], [145], [142], [147], [70], [138], [140], [135], [137], [128], [129].

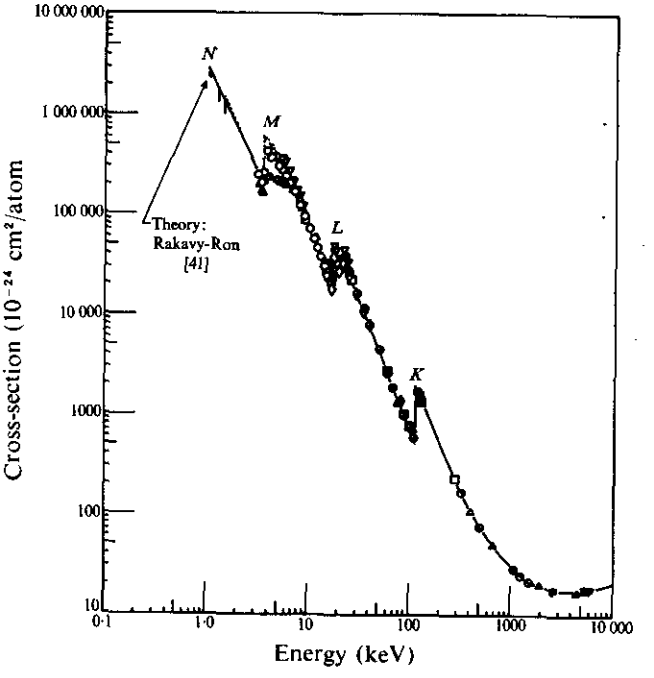

Fig. 2.1.4(6). Total photon interaction cross section, σ_{tot}, for uranium. The theoretical photoeffect results by Rakavy and Ron [41] for this element fall within experimental uncertainties throughout the energy range of measured data. The increasing cross section at high energies results from the transformation of photons into electron–positron pairs, a process which has a threshold of 1022 keV when it takes place in the electrostatic field of an atomic nucleus and 2044 keV in the field of an electron (see, *e.g.*, Motz *et al.* [34]). The experimental values are from [59], [113], [95], [76], [77], [133], [130], [101], [123], [65], [138], [135], [137], [139], [141].

TABLE 2.1A

Wavelengths and Energies Used for Tables 2.1B and 2.1C

Target radiation		Å	keV	Target radiation		Å	keV
Ag	$K\bar{\alpha}$	0·5608	22·105	Ni	$K\bar{\alpha}$	1·6591	7·472
	$K\beta_1$	0·4970	24·942		$K\beta_1$	1·5001	8·265
Pd	$K\bar{\alpha}$	0·5869	21·125	Co	$K\bar{\alpha}$	1·7902	6·925
	$K\beta_1$	0·5205	23·819		$K\beta_1$	1·6208	7·649
Rh	$K\bar{\alpha}$	0·6147	20·169	Fe	$K\bar{\alpha}$	1·9373	6·400
	$K\beta_1$	0·5456	22·724		$K\beta_1$	1·7565	7·058
Mo	$K\bar{\alpha}$	0·7107	17·444	Mn	$K\bar{\alpha}$	2·1031	5·895
	$K\beta_1$	0·6323	19·608		$K\beta_1$	1·9102	6·490
Zn	$K\bar{\alpha}$	1·4364	8·631	Cr	$K\bar{\alpha}$	2·2909	5·412
	$K\beta_1$	1·2952	9·572		$K\beta_1$	2·0848	5·947
Cu	$K\bar{\alpha}$	1·5418	8·041	Ti	$K\bar{\alpha}$	2·7496	4·509
	$K\beta_1$	1·3922	8·905		$K\beta_1$	2·5138	4·932

TABLE 2.1B

Total Cross Section in 10^{-24} cm² per Atom. KA and KB are Identical to $K\bar{\alpha}$ and $K\beta_1$ of Table 2.1A

Radiation	1 Hydrogen	2 Helium	3 Lithium	4 Beryllium	5 Boron	6 Carbon	7 Nitrogen	8 Oxygen
TI KA	.7235	4.392	24.22	84.18	230.6	510.6	999.3	1721
TI KB	.7040	3.657	18.64	63.58	174.0	386.0	758.2	1312
CR KA	.6888	3.089	14.32	47.63	129.8	288.3	568.1	988.0
MN KA	.6782	2.694	11.37	36.70	99.33	220.6	435.7	760.9
CR KB	.6773	2.659	11.11	35.74	96.66	214.6	424.0	740.8
FE KA	.6700	2.404	9.193	28.67	76.85	170.4	337.1	590.6
MN KB	.6688	2.361	8.878	27.51	73.59	163.1	322.7	565.7
CO KA	.6638	2.185	7.594	22.78	60.26	133.3	263.7	463.3
FE KB	.6624	2.140	7.266	21.57	56.86	125.6	248.5	437.0
NI KA	.6588	2.017	6.400	18.38	47.84	105.3	208.3	366.9
CO KB	.6574	1.971	6.088	17.24	44.60	98.02	193.8	341.5
CU KA	.6548	1.884	5.496	15.07	38.45	84.13	166.1	293.1
NI KB	.6533	1.843	5.207	14.01	35.44	77.33	152.6	269.3
ZN KA	.6512	1.783	4.800	12.53	31.23	67.78	133.5	235.7
CU KB	.6497	1.744	4.539	11.58	28.54	61.67	121.3	214.2
ZN KB	.6467	1.663	4.027	9.739	23.28	49.72	97.38	171.8
MO KA	.6238	1.342	2.268	3.668	6.194	10.67	18.37	30.48
MO KB	.6192	1.311	2.150	3.316	5.256	8.546	14.08	22.70
RH KA	.6179	1.304	2.126	3.247	5.075	8.140	13.26	21.21
PD KA	.6155	1.293	2.091	3.149	4.815	7.554	12.08	19.05
AG KA	.6131	1.284	2.061	3.062	4.592	7.054	11.06	17.21
RH KB	.6117	1.278	2.043	3.014	4.469	6.781	10.51	16.21
PD KB	.6093	1.268	2.014	2.939	4.281	6.363	9.673	14.69
AG KB	.6069	1.259	1.988	2.873	4.117	6.005	8.958	13.39

Radiation	9 Fluorine	10 Neon	11 Sodium	12 Magnesium	13 Aluminum	14 Silicon	15 Phosphorus	16 Sulfur
TI KA	2895	4182	6395	8900	11840	15670	19870	24720
TI KB	2218	3213	4939	6905	9214	12260	15630	19390
CR KA	1676	2436	3761	5283	7074	9456	12110	15010
MN KA	1295	1888	2926	4126	5544	7439	9570	11850
CR KB	1262	1840	2851	4023	5407	7258	9341	11570
FE KA	1008	1474	2289	3239	4368	5878	7590	9402
MN KB	966.2	1413	2196	3108	4194	5646	7296	9037
CO KA	792.6	1162	1808	2566	3472	4684	6070	7520
FE KB	748.0	1098	1708	2426	3286	4434	5752	7126
NI KA	628.9	924.6	1441	2050	2784	3764	4894	6065
CO KB	585.7	861.8	1344	1913	2601	3519	4581	5677
CU KA	503.2	741.6	1157	1651	2249	3047	3975	4927
NI KB	462.4	682.2	1065	1520	2074	2810	3670	4551
ZN KA	404.9	598.1	933.3	1334	1824	2473	3236	4016
CU KB	367.9	544.1	848.9	1215	1663	2256	2955	3669
ZN KB	295.1	437.4	682.3	978.1	1344	1825	2396	2979
MO KA	49.99	74.02	112.2	160.7	225.8	304.7	404.8	512.5
MO KB	36.42	53.50	80.11	114.1	160.5	215.7	286.5	364.0
RH KA	33.82	49.57	73.96	105.2	148.0	198.5	263.6	335.2
PD KA	30.04	43.83	64.97	92.05	129.5	173.2	229.9	292.7
AG KA	26.84	38.95	57.34	80.94	113.7	151.8	201.2	256.4
RH KB	25.09	36.30	53.19	74.91	105.2	140.1	185.6	236.7
PD KB	22.44	32.26	46.90	65.75	92.18	122.4	161.9	206.7
AG KB	20.20	28.83	41.56	57.99	81.13	107.3	141.7	181.1

TABLE 2.1B (*continued*)

Total Cross Section in 10^{-24} cm² per Atom. KA and KB are Identical to $K\bar{\alpha}$ and $K\beta_1$ of Table 2.1A

Radiation	17 Chlorine	18 Argon	19 Potassium	20 Calcium	21 Scandium	22 Titanium	23 Vanadium	24 Chromium
TI KA	30500	38260	44060	53540	61170	8858	10560	12330
TI KB	24210	30260	35220	42680	49110	6904	8233	9608
CR KA	18930	23580	27710	33250	38890	45450	6349	7401
MN KA	15080	18730	22200	26520	31340	36520	43370	5822
CR KB	14730	18290	21700	25910	30660	35710	42380	5680
FE KA	12050	14930	17820	21230	25300	29430	34800	39910
MN KB	11590	14360	17160	20440	24390	28370	33510	38460
CO KA	9696	11990	14410	17130	20570	23900	28140	32380
FE KB	9202	11380	13690	16270	19570	22720	26740	30790
NI KA	7868	9715	11750	13930	16850	19550	22940	26470
CO KB	7378	9105	11030	13070	15840	18370	21540	24880
CU KA	6429	7924	9637	11410	13890	16100	18830	21780
NI KB	5947	7327	8927	10570	12880	14930	17450	20210
ZN KA	5261	6476	7912	9365	11450	13270	15490	17960
CU KB	4815	5925	7252	8584	10510	12190	14210	16500
ZN KB	3926	4824	5932	7020	8631	10010	11640	13550
MO KA	685.3	837.0	1052	1264	1571	1849	2135	2526
MO KB	486.4	593.5	747.5	902.7	1120	1324	1528	1813
RH KA	447.8	546.2	688.2	832.1	1032	1221	1410	1673
PD KA	390.5	476.2	599.9	726.9	899.7	1067	1232	1464
AG KA	341.6	416.5	524.6	637.1	787.2	935.5	1081	1285
RH KB	315.1	384.0	483.5	588.0	725.8	863.6	998.0	1187
PD KB	274.6	334.5	421.1	513.2	632.3	753.7	871.4	1037
AG KB	240.2	292.4	367.9	449.3	552.6	660.0	763.2	908.7

Radiation	25 Manganese	26 Iron	27 Cobalt	28 Nickel	29 Copper	30 Zinc	31 Gallium	32 Germanium
TI KA	14600	17460	20140	23370	27140	30400	35790	39680
TI KB	11380	13620	15760	18310	21190	23910	27980	31070
CR KA	8765	10490	12190	14190	16380	18640	21640	24100
MN KA	6895	8248	9630	11230	12920	14830	17080	19080
CR KB	6728	8047	9399	10960	12610	14490	16670	18630
FE KA	5467	6528	7661	8942	10270	11900	13580	15240
MN KB	5256	6274	7368	8602	9878	11460	13060	14670
CO KA	36960	5216	6151	7187	8241	9630	10900	12290
FE KB	35140	4942	5834	6819	7815	9152	10340	11670
NI KA	30210	33990	4981	5826	6668	7858	8820	9992
CO KB	28390	32040	4669	5462	6248	7382	8264	9376
CU KA	24860	28230	33130	4759	5437	6460	7193	8186
NI KB	23080	26280	30810	4409	5035	6002	6658	7596
ZN KA	20520	23490	27490	29830	4460	5345	5895	6750
CU KB	18850	21660	25310	27560	4088	4917	5401	6201
ZN KB	15500	17960	20920	22950	25880	4056	4413	5097
MO KA	2906	3500	4014	4604	5206	6021	6587	7289
MO KB	2088	2523	2888	3331	3774	4370	4826	5335
RH KA	1927	2330	2666	3079	3490	4042	4473	4943
PD KA	1687	2040	2333	2697	3061	3545	3931	4345
AG KA	1481	1791	2047	2370	2693	3118	3465	3830
RH KB	1368	1654	1891	2191	2491	2884	3209	3547
PD KB	1196	1446	1652	1916	2181	2525	2816	3113
AG KB	1048	1267	1447	1681	1915	2217	2478	2739

TABLE 2.1B (*continued*)

Total Cross Section in 10^{-24} cm² per Atom. KA and KB are Identical to $K\bar{\alpha}$ and $K\beta_1$ of Table 2.1A

Radiation	33 Arsenic	34 Selenium	35 Bromine	36 Krypton	37 Rubidium	38 Strontium	39 Yttrium	40 Zirconium
TI KA	45710	52830	57740	64610	72120	80320	88360	98120
TI KB	35880	41520	45410	50860	56810	63360	69750	77390
CR KA	27860	32260	35320	39600	44240	49370	54450	60370
MN KA	22080	25570	28020	31450	35140	39230	43350	48020
CR KB	21560	24970	27370	30710	34320	38310	42340	46910
FE KA	17610	20390	22380	25140	28090	31340	34730	38440
MN KB	16950	19620	21540	24200	27040	30160	33440	37010
CO KA	14180	16400	18030	20270	22660	25250	28070	31040
FE KB	13460	15560	17110	19250	21510	23970	26660	29480
NI KA	11510	13300	14640	16480	18420	20510	22870	25270
CO KB	10790	12470	13740	15470	17280	19240	21470	23720
CU KA	9411	10870	11980	13500	15090	16780	18760	20710
NI KB	8720	10060	11100	12510	13980	15540	17410	19210
ZN KA	7733	8915	9848	11100	12400	13770	15460	17050
CU KB	7092	8171	9033	10190	11380	12620	14200	15650
ZN KB	5809	6682	7401	8353	9325	10330	11660	12840
MO KA	8207	9023	9910	11010	11780	12810	14400	2439
MO KB	6042	6713	7373	8159	8809	9543	10710	11390
RH KA	5605	6242	6857	7582	8202	8880	9964	10610
PD KA	4933	5512	6055	6690	7255	7855	8814	9412
AG KA	4354	4881	5362	5918	6434	6967	7817	8367
RH KB	4035	4533	4980	5493	5981	6477	7267	7789
PD KB	3545	3996	4390	4838	5281	5719	6417	6895
AG KB	3123	3532	3881	4274	4676	5064	5681	6120

Radiation	41 Niobium	42 Molybdenum	43 Technetium	44 Ruthenium	45 Rhodium	46 Palladium	47 Silver	48 Cadmium
TI KA	107500	117600	129200	139600	152400	163900	176800	198600
TI KB	85170	93140	102100	110900	121000	130500	140700	157100
CR KA	66630	72880	79810	86940	94860	102600	110600	122900
MN KA	53120	58120	63600	69480	75820	82250	88610	98090
CR KB	51900	56790	62140	67890	74100	80400	86620	95840
FE KA	42560	46610	50990	55820	60940	66230	71370	78770
MN KB	40980	44890	49100	53770	58710	63820	68790	75880
CO KA	34380	37690	41220	45220	49380	53760	57960	63790
FE KB	32660	35810	39170	42980	46940	51120	55120	60630
NI KA	28000	30720	33590	36920	40330	43970	47420	52060
CO KB	26280	28840	31540	34680	37890	41330	44580	48910
CU KA	22960	25210	27570	30350	33170	36210	39070	42790
NI KB	21280	23380	25580	28160	30780	33620	36290	39730
ZN KA	18880	20770	22720	25030	27370	29910	32300	35330
CU KB	17320	19060	20860	22990	25140	27490	29700	32470
ZN KB	14200	15650	171.30	18900	20670	22630	24470	26710
MO KA	2617	2937	3251	3581	3938	4314	4725	5175
MO KB	12530	2118	2350	2585	2845	3114	3422	3756
RH KA	11670	12640	2173	2389	2630	2878	3165	3477
PD KA	10350	11210	12000	2398	2310	2525	2780	3058
AG KA	9200	9963	10680	1847	2035	2222	2449	2698
RH KB	8564	9275	9954	10710	1884	2056	2268	2500
PD KB	7581	8210	8826	9500	9975	1802	1990	2197
AG KB	6729	7286	7845	8450	8889	10080	1752	1936

TABLE 2.1B *(continued)*

Total Cross Section in 10^{-24} cm² per Atom. KA and KB are Identical to $K\bar{\alpha}$ and $K\beta_1$ of Table 2.1A

Radiation	49 Indium	50 Tin	51 Antimony	52 Tellurium	53 Iodine	54 Xenon	55 Cesium	56 Barium
TI KA	219400	222400	201600	159600	61720	65340	71380	76130
TI KB	172600	177200	187200	178600	194000	148800	57070	60690
CR KA	134500	139700	148300	162900	176000	164700	177100	134000
MN KA	107000	112200	119700	130600	140300	152800	163800	150500
CR KB	104500	109700	117100	127700	137100	149400	160000	147100
FE KA	85620	90600	96950	105400	112800	123100	131700	140300
MN KB	82440	87350	93520	101600	108700	118700	126900	135200
CO KA	69140	73740	79140	85680	91450	100100	106800	113800
FE KB	65670	70170	75360	81520	86930	95180	101500	108300
NI KA	56280	60470	65090	70210	74710	81930	87240	93100
CO KB	52820	56890	61290	66040	70210	77040	81990	87510
CU KA	46140	49930	53890	57930	61470	67540	71800	76670
NI KB	42810	46410	50120	53840	57100	62760	66700	71260
ZN KA	38040	41350	44710	47970	50840	55910	59390	63480
CU KB	34930	38050	41180	44150	46760	51440	54620	58410
ZN KB	28700	31410	34050	36430	38540	42430	45020	48200
MO KA	5554	6145	6675	7186	7654	8352	8923	9665
MO KB	4037	4459	4837	5227	5590	6075	6511	7071
RH KA	3738	4125	4472	4839	5182	5624	6034	6557
PD KA	3291	3623	3921	4256	4570	4947	5319	5788
AG KA	2906	3191	3449	3753	4042	4364	4702	5123
RH KB	2694	2955	3190	3478	3751	4043	4363	4756
PD KB	2370	2592	2794	3055	3304	3552	3841	4193
AG KB	2091	2281	2455	2692	2919	3130	3392	3707

Radiation	57 Lanthanum	58 Cerium	59 Praseodymium	60 Neodymium	61 Promethium	62 Samarium	63 Europium	64 Gadolinium
TI KA	81800	88990	96820	103600	110900	118000	126900	133300
TI KB	65100	70810	77110	82400	88160	93610	100500	105800
CR KA	51400	55920	60940	65000	69500	73680	78920	83280
MN KA	156000	121200	49100	52280	55870	59130	63230	66860
CR KB	152600	118500	48020	51120	54630	57810	61800	65370
FE KA	146600	137800	105300	111100	45300	47880	51100	54150
MN KB	141400	132900	142700	107100	116100	46200	49290	52250
CO KA	119700	130100	139500	127400	97970	102800	41690	44260
FE KB	114000	123800	132700	121300	130900	97880	106000	42160
NI KA	98450	106700	114200	121200	130600	118500	91200	96320
CO KB	92700	100400	107300	114000	122800	111500	120400	90560
CU KA	81520	88120	94090	100100	107700	113200	105500	111400
NI KB	75870	81970	87480	93170	100100	105300	113600	103700
ZN KA	67750	73140	77980	83160	89210	93970	101200	107000
CU KB	62440	67370	71780	76610	82110	86540	93140	98530
ZN KB	51720	55730	59280	63400	67800	71570	76890	81350
MO KA	10460	11300	11880	12770	13550	14470	15440	16400
MO KB	7635	8267	8679	9316	9891	10590	11290	12000
RH KA	7074	7666	8044	8631	9165	9819	10470	11130
PD KA	6229	6764	7092	7602	8077	8663	9240	9825
AG KA	5501	5984	6271	6714	7139	7664	8177	8698
RH KB	5101	5555	5819	6226	6623	7114	7592	8076
PD KB	4485	4896	5123	5476	5829	6268	6691	7119
AG KB	3956	4325	4525	4830	5145	5538	5914	6294

TABLE 2.1B *(continued)*

Total Cross Section in 10^{-24} cm² per Atom. KA and KB are Identical to $K\bar{\alpha}$ and $K\beta_1$ of Table 2.1A

Radiation	65 Terbium	66 Dysprosium	67 Holmium	68 Erbium	69 Thulium	70 Ytterbium	71 Lutetium	72 Hafnium
TI KA	144000	153200	161300	170900	180600	190800	202200	213500
TI KB	113900	121000	127200	134800	142400	150400	159500	168500
CR KA	89420	94910	99490	105500	111400	117700	124800	131900
MN KA	71600	75910	79400	84180	88860	93900	99640	105300
CR KB	69980	74190	77590	82250	86830	91750	97360	102900
FE KA	57840	61260	63940	67800	71550	75610	80270	84870
MN KB	55780	59070	61640	65350	68970	72890	77370	81820
CO KA	47160	49900	51980	55120	58150	61460	65260	69030
FE KB	44900	47490	49450	52440	55320	58470	62090	65680
NI KA	38760	40960	42590	45170	47640	50360	53490	56590
CO KB	96870	38550	40060	42490	44810	47370	50320	53240
CU KA	84940	90830	35160	37300	39320	41570	44170	46740
NI KB	110900	84430	91220	34710	36600	38690	41110	43520
ZN KA	98960	105600	81140	88250	32690	34550	36730	38880
CU KB	105500	97190	74570	81030	80900	31850	33870	35850
ZN KB	87160	92810	99680	93320	66920	66510	71640	69940
MO KA	17620	18590	19750	21000	22150	23050	24460	25590
MO KB	12900	13590	14450	15300	16250	17010	18030	19010
RH KA	11960	12600	13400	14170	15080	15810	16750	17690
PD KA	10560	11130	11840	12510	13330	13990	14820	15660
AG KA	9345	9853	10490	11060	11810	12410	13160	13910
RH KB	8677	9150	9746	10270	10980	11540	12230	12940
PD KB	7649	8068	8599	9047	9688	10200	10810	11440
AG KB	6762	7134	7609	7993	8575	9037	9584	10150

Radiation	73 Tantalum	74 Tungsten	75 Rhenium	76 Osmium	77 Iridium	78 Platinum	79 Gold	80 Mercury
TI KA	221100	230000	246200	260400	278000	302700	296500	319200
TI KB	174500	182500	195000	206100	219700	237700	235800	253100
CR KA	136700	143600	153200	161800	172200	185200	186000	199100
MN KA	109200	115300	122700	129600	137700	147200	149600	159800
CR KB	106700	112700	120000	126700	134500	143800	146300	156200
FE KA	88010	93350	99220	104700	111100	118100	121300	129300
MN KB	84850	90060	95700	101000	107100	113800	117100	124700
CO KA	71610	76260	80950	85350	90430	95640	99310	105600
FE KB	68140	72640	77070	81250	86060	90900	94630	100600
NI KA	58730	62790	66550	70120	74210	78070	81900	86880
CO KB	55260	59140	62670	66010	69830	73340	77190	81830
CU KA	48530	52070	55120	58030	61350	64210	68030	72010
NI KB	45190	48550	51370	54070	57130	59680	63460	67130
ZN KA	40380	43480	45970	48370	51060	53200	56890	60100
CU KB	37240	40160	42440	44640	47100	48970	52580	55490
ZN KB	30900	33440	35290	37100	39090	40450	43850	46180
MO KA	26900	29240	30530	31660	32990	35180	36450	38210
MO KB	19860	21550	22410	23410	24640	25990	26960	28410
RH KA	18450	20010	20800	21760	22950	24150	25060	26440
PD KA	16340	17700	18400	19280	20360	21380	22200	23450
AG KA	14500	15690	16320	17130	18110	18980	19710	20860
RH KB	13490	14590	15170	15940	16870	17650	18340	19420
PD KB	11920	12880	13400	14100	14940	15600	16220	17200
AG KB	10570	11400	11870	12510	13270	13830	14390	15280

TABLE 2.1B *(continued)*

Total Cross Section in 10^{-24} cm² per Atom. KA and KB are Identical to $K\bar{\alpha}$ and $K\beta_1$ of Table 2.1A

Radiation	81 Thallium	82 Lead	83 Bismuth	86 Radon	90 Thorium	92 Uranium	94 Plutonium
TI KA	336200	356000	369800	432600	423100	428400	381000
TI KB	266400	282100	293800	342900	382400	340900	406000
CR KA	209400	221700	231500	269600	325200	306000	318900
MN KA	167800	177700	186000	216100	261200	265700	290400
CR KB	164000	173700	181900	211300	255400	259800	306100
FE KA	135700	143700	150800	174800	211600	215600	253100
MN KB	130900	138600	145500	168600	204200	208000	244100
CO KA	110700	117200	123300	142700	173000	176500	206300
FE KB	105400	111600	117400	135900	164800	168100	196400
NI KA	91060	96400	101600	117300	142500	145500	169400
CO KB	85750	90770	95700	110500	134200	137200	159400
CU KA	75430	79840	84290	97190	118200	120900	140100
NI KB	70290	74400	78600	90580	110200	112700	130500
ZN KA	62900	66580	70420	81060	98680	101000	116700
CU KB	58070	61460	65060	74830	91140	93380	107700
ZN KB	48280	51100	54190	62220	75880	77830	89390
MO KA	40530	42230	43680	43180	38320	38220	19390
MO KB	29950	31150	32450	37130	28250	28720	31360
RH KA	27840	28940	30190	34570	36600	26800	29260
PD KA	24670	25630	26800	30700	37440	33300	26090
AG KA	21910	22760	23850	27330	33240	34360	23330
RH KB	20390	21170	22220	25460	30920	32070	30320
PD KB	18040	18710	19690	22580	27330	28500	31100
AG KB	16000	16590	17500	20070	24220	25400	27690

TABLE 2.1C

Mass Attenuation Coefficients (μ/ρ) in $cm^2\ g^{-1}$

Radiation	1 Hydrogen	2 Helium	3 Lithium	4 Beryllium	5 Boron	6 Carbon	7 Nitrogen	8 Oxygen
TI KA	.4323	.6607	2.102	5.625	12.85	25.60	42.96	64.79
TI KB	.4206	.5503	1.617	4.249	9.693	19.36	32.59	49.40
CR KA	.4116	.4648	1.243	3.183	7.232	14.46	24.42	37.19
MN KA	.4052	.4054	.9863	2.452	5.534	11.06	18.73	28.64
CR KB	.4046	.4001	.9639	2.388	5.385	10.76	18.23	27.88
FE KA	.4003	.3616	.7977	1.916	4.282	8.547	14.49	22.23
MN KB	.3996	.3553	.7704	1.839	4.100	8.181	13.87	21.29
CO KA	.3966	.3288	.6590	1.522	3.357	6.683	11.33	17.44
FE KB	.3958	.3219	.6306	1.442	3.168	6.299	10.68	16.45
NI KA	.3936	.3034	.5554	1.228	2.665	5.282	8.955	13.81
CO KB	.3928	.2966	.5283	1.152	2.485	4.916	8.330	12.85
CU KA	.3912	.2835	.4770	1.007	2.142	4.219	7.142	11.03
NI KB	.3903	.2772	.4518	.9363	1.975	3.878	6.560	10.14
ZN KA	.3891	.2682	.4165	.8373	1.740	3.399	5.740	8.873
CU KB	.3882	.2623	.3939	.7742	1.590	3.093	5.215	8.062
ZN KB	.3864	.2503	.3494	.6509	1.297	2.493	4.186	6.468
MO KA	.3727	.2019	.1968	.2451	.3451	.5348	.7898	1.147
MO KB	.3699	.1972	.1866	.2216	.2928	.4285	.6054	.8545
RH KA	.3692	.1961	.1845	.2170	.2827	.4082	.5702	.7985
PD KA	.3677	.1946	.1815	.2104	.2683	.3788	.5191	.7171
AG KA	.3663	.1931	.1788	.2047	.2558	.3537	.4756	.6479
RH KB	.3655	.1923	.1773	.2014	.2490	.3400	.4519	.6102
PD KB	.3640	.1908	.1748	.1964	.2385	.3191	.4158	.5529
AG KB	.3626	.1894	.1726	.1920	.2294	.3011	.3851	.5041

Radiation	9 Fluorine	10 Neon	11 Sodium	12 Magnesium	13 Aluminum	14 Silicon	15 Phosphorus	16 Sulfur
TI KA	91.76	124.8	167.5	220.4	264.4	336.0	386.3	464.2
TI KB	70.30	95.88	129.3	171.0	205.8	262.9	303.9	364.2
CR KA	53.14	72.71	98.48	130.8	158.0	202.7	235.5	281.9
MN KA	41.06	56.36	76.61	102.2	123.8	159.5	186.0	222.6
CR KB	39.99	54.91	74.66	99.62	120.7	155.6	181.6	217.2
FE KA	31.96	44.00	59.94	80.21	97.54	126.0	147.6	176.6
MN KB	30.62	42.18	57.49	76.97	93.65	121.0	141.8	169.7
CO KA	25.12	34.69	47.34	63.54	77.54	100.4	118.0	141.2
FE KB	23.71	32.75	44.73	60.06	73.37	95.07	111.8	133.8
NI KA	19.93	27.59	37.73	50.77	62.17	80.69	95.15	113.9
CO KB	18.57	25.72	35.18	47.38	58.08	75.44	89.05	106.6
CU KA	15.95	22.13	30.30	40.88	50.23	65.32	77.28	92.53
NI KB	14.66	20.36	27.87	37.64	46.30	60.24	71.34	85.47
ZN KA	12.83	17.85	24.44	33.04	40.73	53.03	62.90	75.41
CU KB	11.66	16.24	22.23	30.08	37.14	48.37	57.44	68.90
ZN KB	9.355	13.05	17.87	24.22	30.01	39.12	46.58	55.94
MO KA	1.584	2.209	2.939	3.979	5.043	6.533	7.870	9.625
MO KB	1.154	1.597	2.098	2.825	3.585	4.624	5.569	6.835
RH KA	1.072	1.479	1.937	2.604	3.304	4.256	5.125	6.295
PD KA	.9523	1.308	1.701	2.280	2.891	3.714	4.468	5.496
AG KA	.8507	1.163	1.501	2.004	2.540	3.254	3.911	4.816
RH KB	.7954	1.083	1.393	1.855	2.349	3.003	3.607	4.445
PD KB	.7114	.9629	1.228	1.628	2.058	2.623	3.146	3.881
AG KB	.6401	.8605	1.088	1.436	1.812	2.301	2.755	3.401

TABLE 2.1C *(continued)*

Mass Attenuation Coefficients (μ/ρ) in cm^2 g^{-1}

Radiation	17 Chlorine	18 Argon	19 Potassium	20 Calcium	21 Scandium	22 Titanium	23 Vanadium	24 Chromium
TI KA	518.1	576.9	678.7	804.5	819.4	111.4	124.9	142.8
TI KB	411.1	456.2	542.4	638.3	657.8	86.80	97.33	111.3
CR KA	321.5	355.5	426.8	499.6	520.9	571.4	75.06	85.71
MN KA	256.1	282.4	341.9	398.4	419.8	459.2	512.7	67.43
CR KB	250.2	275.8	334.2	389.3	410.7	449.0	501.0	65.79
FE KA	204.6	225.1	274.5	319.0	338.9	370.1	411.4	462.2
MN KB	196.9	216.5	264.4	307.1	326.7	356.7	396.2	445.4
CO KA	164.7	180.9	222.0	257.4	275.5	300.5	332.7	375.0
FE KB	156.3	171.6	210.9	244.4	262.1	285.7	316.1	356.6
NI KA	133.6	146.5	180.9	209.3	225.6	245.8	271.2	306.6
CO KB	125.3	137.3	169.9	196.4	212.2	231.0	254.7	288.1
CU KA	109.2	119.5	148.4	171.4	186.0	202.4	222.6	252.3
NI KB	101.0	110.5	137.5	158.8	172.6	187.8	206.3	234.1
ZN KA	89.35	97.65	121.9	140.7	153.3	166.9	183.1	208.0
CU KB	81.79	89.34	111.7	129.0	140.8	153.2	168.0	191.1
ZN KB	66.68	72.74	91.36	105.5	115.6	125.9	137.7	157.0
MO KA	11.64	12.62	16.20	19.00	21.04	23.25	25.24	29.25
MO KB	8.261	8.949	11.51	13.56	15.00	16.65	18.07	20.99
RH KA	7.605	8.237	10.60	12.50	13.82	15.35	16.66	19.37
PD KA	6.632	7.180	9.240	10.92	12.05	13.42	14.57	16.95
AG KA	5.803	6.280	8.080	9.573	10.54	11.76	12.78	14.88
RH KB	5.351	5.790	7.448	8.836	9.723	10.86	11.80	13.74
PD KB	4.663	5.044	6.486	7.711	8.469	9.477	10.30	12.01
AG KB	4.079	4.409	5.667	6.752	7.402	8.298	9.024	10.52

Radiation	25 Manganese	26 Iron	27 Cobalt	28 Nickel	29 Copper	30 Zinc	31 Gallium	32 Germanium
TI KA	160.0	188.3	205.8	239.8	257.2	280.0	309.1	329.2
TI KB	124.7	146.9	161.0	187.9	200.9	220.3	241.7	257.8
CR KA	96.08	113.1	124.6	145.7	155.2	171.7	186.9	199.9
MN KA	75.59	88.94	98.41	115.2	122.5	136.6	147.6	158.3
CR KB	73.75	86.77	96.06	112.5	119.5	133.5	144.0	154.5
FE KA	59.93	70.40	78.29	91.76	97.36	109.6	117.3	126.4
MN KB	57.62	67.65	75.30	88.27	93.63	105.6	112.8	121.7
CO KA	405.1	56.25	62.86	73.75	78.11	88.71	94.15	102.0
FE KB	385.2	53.29	59.63	69.97	74.07	84.30	89.29	96.81
NI KA	331.2	366.5	50.91	59.78	63.20	72.38	76.19	82.90
CO KB	311.2	345.5	47.71	56.05	59.22	68.00	71.39	77.79
CU KA	272.5	304.4	338.6	48.83	51.54	59.51	62.13	67.92
NI KB	253.0	283.4	314.9	45.24	47.72	55.29	57.51	63.02
ZN KA	224.9	253.3	280.9	306.1	42.28	49.24	50.92	56.01
CU KB	206.7	233.6	258.7	282.8	38.74	45.30	46.65	51.44
ZN KB	169.9	193.7	213.8	235.5	245.3	37.37	38.12	42.29
MO KA	31.86	37.74	41.02	47.24	49.34	55.46	56.90	60.47
MO KB	22.89	27.21	29.51	34.18	35.77	40.26	41.69	44.26
RH KA	21.12	25.13	27.24	31.60	33.08	37.23	38.64	41.01
PD KA	18.49	21.99	23.84	27.68	29.02	32.65	33.96	36.05
AG KA	16.23	19.31	20.92	24.32	25.52	28.72	29.93	31.78
RH KB	15.00	17.84	19.32	22.48	23.61	26.56	27.72	29.43
PD KB	13.11	15.59	16.88	19.66	20.67	23.26	24.32	25.82
AG KB	11.49	13.67	14.79	17.25	18.15	20.42	21.41	22.73

TABLE 2.1C (*continued*)

Mass Attenuation Coefficients (μ/ρ) in $cm^2\ g^{-1}$

Radiation	33 Arsenic	34 Selenium	35 Bromine	36 Krypton	37 Rubidium	38 Strontium	39 Yttrium	40 Zirconium
TI KA	367.5	402.9	435.1	464.3	508.1	552.1	598.6	647.8
TI KB	288.4	316.7	342.2	365.5	400.3	435.5	472.5	510.9
CR KA	224.0	246.1	266.2	284.6	311.7	339.3	368.9	398.6
MN KA	177.5	195.0	211.2	226.0	247.6	269.6	293.7	317.1
CR KB	173.3	190.4	206.2	220.7	241.8	263.4	286.9	309.7
FE KA	141.6	155.5	168.6	180.7	197.9	215.4	235.3	253.8
MN KB	136.2	149.6	162.3	173.9	190.5	207.3	226.6	244.4
CO KA	114.0	125.1	135.8	145.7	159.6	173.5	190.2	204.9
FE KB	108.2	118.7	129.0	138.3	151.6	164.7	180.6	194.6
NI KA	92.51	101.4	110.3	118.5	129.8	140.9	154.9	166.8
CO KB	86.76	95.11	103.5	111.2	121.8	132.2	145.4	156.6
CU KA	75.65	82.89	90.29	97.02	106.3	115.3	127.1	136.8
NI KB	70.10	76.75	83.67	89.94	98.50	106.8	117.9	126.8
ZN KA	62.16	68.00	74.21	79.80	87.39	94.66	104.8	112.6
CU KB	57.01	62.32	68.07	73.22	80.16	86.77	96.19	103.3
ZN KB	46.70	50.97	55.77	60.03	65.70	70.99	79.01	84.77
MO KA	65.97	68.82	74.68	79.10	83.00	88.04	97.56	16.10
MO KB	48.57	51.20	55.56	58.64	62.07	65.59	72.57	75.20
RH KA	45.06	47.61	51.67	54.49	57.79	61.03	67.50	70.07
PD KA	39.66	42.05	45.63	48.08	51.11	53.99	59.71	62.14
AG KA	35.00	37.23	40.41	42.53	45.33	47.89	52.96	55.24
RH KB	32.44	34.57	37.52	39.48	42.14	44.52	49.23	51.43
PD KB	28.50	30.48	33.08	34.77	37.21	39.31	43.47	45.52
AG KB	25.11	26.94	29.24	30.71	32.94	34.81	38.49	40.40

Radiation	41 Niobium	42 Molybdenum	43 Technetium	44 Ruthenium	45 Rhodium	46 Palladium	47 Silver	48 Cadmium
TI KA	696.9	738.4	785.8	831.9	892.0	927.9	986.9	1064
TI KB	552.1	584.6	621.2	660.4	707.9	738.5	785.2	841.8
CR KA	431.9	457.4	485.5	517.9	555.2	580.9	617.4	658.8
MN KA	344.3	364.8	386.9	413.9	443.8	465.5	494.6	525.6
CR KB	336.4	356.5	378.0	404.4	433.7	455.1	483.5	513.5
FE KA	275.9	292.6	310.2	332.5	356.7	374.9	398.4	422.0
MN KB	265.7	281.7	298.7	320.3	343.6	361.3	383.9	406.6
CO KA	222.9	236.6	250.8	269.4	289.0	304.3	323.5	341.8
FE KB	211.7	224.8	238.3	256.0	274.7	289.3	307.6	324.8
NI KA	181.5	192.8	204.4	219.9	236.0	248.9	264.7	279.0
CO KB	170.4	181.0	191.9	206.6	221.8	234.0	248.9	262.1
CU KA	148.8	158.3	167.7	180.8	194.1	205.0	218.1	229.3
NI KB	138.0	146.8	155.6	167.8	180.2	190.3	202.5	212.9
ZN KA	122.4	130.3	138.2	149.1	160.2	169.3	180.3	189.3
CU KB	112.3	119.7	126.9	137.0	147.1	155.6	165.8	174.0
ZN KB	92.04	98.23	104.2	112.6	121.0	128.1	136.6	143.1
MO KA	16.96	18.44	19.78	21.33	23.05	24.42	26.38	27.73
MO KB	81.22	13.29	14.30	15.40	16.65	17.63	19.10	20.13
RH KA	75.64	79.32	13.22	14.23	15.39	16.29	17.67	18.63
PD KA	67.08	70.34	72.99	12.50	13.52	14.29	15.52	16.38
AG KA	59.63	62.53	64.99	11.00	11.91	12.58	13.67	14.45
RH KB	55.51	58.21	60.56	63.80	11.03	11.64	12.66	13.40
PD KB	49.14	51.53	53.69	56.59	58.38	10.20	11.11	11.77
AG KB	43.62	45.73	47.73	50.34	52.03	57.03	9.780	10.37

TABLE 2.1C *(continued)*

Mass Attenuation Coefficients (μ/ρ) in cm² g⁻¹

Radiation	49 Indium	50 Tin	51 Antimony	52 Tellurium	53 Iodine	54 Xenon	55 Cesium	56 Barium
TI KA	1151	1128	996.7	753.3	292.9	299.7	323.5	333.7
TI KB	905.6	899.1	925.7	842.9	920.9	682.7	258.6	266.0
CR KA	705.8	708.8	733.4	768.9	835.2	755.4	802.7	587.3
MN KA	561.1	569.3	591.7	616.6	666.1	701.0	742.2	659.7
CR KB	548.0	556.6	578.8	602.7	650.8	685.2	725.1	644.6
FE KA	449.2	459.7	479.4	497.3	535.3	564.9	596.6	614.9
MN KB	432.5	443.2	462.4	479.4	515.8	544.5	574.9	592.5
CO KA	362.7	374.1	391.3	404.4	434.0	459.0	483.8	499.0
FE KB	344.5	356.0	372.6	384.7	412.6	436.6	460.0	474.5
NI KA	295.2	306.8	321.9	331.4	354.6	375.8	395.4	408.1
CO KB	277.1	288.7	303.1	311.7	333.2	353.4	371.5	383.6
CU KA	242.1	253.3	266.5	273.4	291.7	309.8	325.4	336.1
NI KB	224.6	235.5	247.8	254.1	271.0	287.9	302.3	312.3
ZN KA	199.5	209.8	221.1	226.4	241.3	256.4	269.1	278.3
CU KB	183.3	193.1	203.6	208.4	221.9	235.9	247.5	256.0
ZN KB	150.6	159.3	168.3	172.0	182.9	194.6	204.0	211.3
MO KA	29.13	31.18	33.01	33.92	36.33	38.31	40.44	42.37
MO KB	21.18	22.62	23.91	24.67	26.53	27.86	29.51	31.00
RH KA	19.61	20.93	22.11	22.84	24.59	25.80	27.34	28.74
PD KA	17.26	18.38	19.39	20.09	21.69	22.69	24.10	25.37
AG KA	15.25	16.19	17.05	17.72	19.18	20.01	21.31	22.45
RH KB	14.14	14.99	15.77	16.41	17.80	18.55	19.77	20.85
PD KB	12.43	13.15	13.82	14.42	15.68	16.29	17.41	18.38
AG KB	10.97	11.57	12.14	12.70	13.85	14.36	15.37	16.25

Radiation	57 Lanthanum	58 Cerium	59 Praseodymium	60 Neodymium	61 Promethium	62 Samarium	63 Europium	64 Gadolinium
TI KA	354.7	382.6	413.8	432.5	454.6	472.6	502.8	510.4
TI KB	282.3	304.4	329.6	343.9	361.2	374.9	398.1	405.0
CR KA	222.9	240.4	260.5	271.3	284.7	295.0	312.7	318.9
MN KA	676.5	521.1	209.9	218.2	228.9	236.8	250.5	256.0
CR KB	661.5	509.4	205.3	213.4	223.8	231.5	244.9	250.3
FE KA	635.6	592.3	450.1	463.5	185.6	191.7	202.5	207.3
MN KB	613.2	571.2	609.7	447.2	475.7	185.0	195.3	200.0
CO KA	519.0	559.1	596.2	531.7	401.4	411.8	165.2	169.5
FE KB	494.2	532.1	567.0	506.2	536.4	392.0	419.9	161.4
NI KA	426.9	458.6	488.0	505.8	535.2	474.6	361.3	368.8
CO KB	401.9	431.5	458.8	475.9	503.2	446.3	476.9	346.7
CU KA	353.5	378.8	402.2	417.9	441.1	453.5	417.9	426.7
NI KB	329.0	352.4	373.9	388.8	410.0	421.8	449.9	396.9
ZN KA	293.8	314.4	333.3	347.1	365.5	376.3	401.0	409.8
CU KB	270.8	289.6	306.8	319.8	336.4	346.6	369.0	377.2
ZN KB	224.3	239.6	253.4	264.6	277.8	286.6	304.7	311.5
MO KA	45.34	48.56	50.78	53.28	55.52	57.96	61.18	62.79
MO KB	33.10	35.54	37.09	38.88	40.52	42.40	44.74	45.95
RH KA	30.67	32.96	34.38	36.02	37.55	39.32	41.48	42.61
PD KA	27.01	29.07	30.31	31.73	33.09	34.69	36.61	37.62
AG KA	23.85	25.72	26.80	28.02	29.25	30.69	32.40	33.30
RH KB	22.12	23.88	24.87	25.98	27.13	28.49	30.08	30.92
PD KB	19.45	21.04	21.90	22.85	23.88	25.10	26.51	27.26
AG KB	17.15	18.59	19.34	20.16	21.08	22.18	23.43	24.10

TABLE 2.1C (*continued*)

Mass Attenuation Coefficients (μ/ρ) in $cm^2\ g^{-1}$

Radiation	65 Terbium	66 Dysprosium	67 Holmium	68 Erbium	69 Thulium	70 Ytterbium	71 Lutetium	72 Hafnium
TI KA	545.7	567.7	589.2	615.3	643.9	664.1	695.8	720.2
TI KB	431.7	448.6	464.5	485.3	507.6	523.7	548.9	568.4
CR KA	338.9	351.7	363.3	379.7	397.0	409.6	429.5	445.0
MN KA	271.4	281.3	290.0	303.0	316.9	326.9	342.9	355.3
CR KB	265.2	275.0	283.4	296.1	309.6	319.4	335.1	347.2
FE KA	219.2	227.0	233.5	244.1	255.1	263.2	276.2	286.4
MN KB	211.4	218.9	225.1	235.3	245.9	253.7	266.3	276.1
CO KA	178.7	184.9	189.8	198.4	207.4	214.0	224.6	232.9
FE KB	170.2	176.0	180.6	188.8	197.3	203.5	213.7	221.6
NI KA	146.9	151.8	155.5	162.6	169.9	175.3	184.1	190.9
CO KB	367.1	142.9	146.3	153.0	159.8	164.9	173.2	179.6
CU KA	321.9	336.6	128.4	134.3	140.2	144.7	152.0	157.7
NI KB	420.4	312.9	333.2	125.0	130.5	134.7	141.5	146.8
ZN KA	375.1	391.5	296.3	317.7	116.6	120.3	126.4	131.2
CU KB	399.9	360.2	272.4	291.7	288.5	110.9	116.5	121.0
ZN KB	330.3	344.0	364.0	335.9	238.6	231.5	246.6	236.0
MO KA	66.77	68.89	72.14	75.61	78.98	80.23	84.18	86.33
MO KB	48.88	50.38	52.76	55.07	57.94	59.22	62.04	64.15
RH KA	45.33	46.71	48.93	51.03	53.77	55.03	57.63	59.68
PD KA	40.01	41.24	43.23	45.02	47.52	48.70	51.01	52.85
AG KA	35.42	36.52	38.31	39.83	42.12	43.21	45.27	46.93
RH KB	32.89	33.91	35.59	36.97	39.14	40.18	42.11	43.66
PD KB	28.99	29.90	31.41	32.57	34.54	35.50	37.21	38.61
AG KB	25.63	26.44	27.79	28.77	30.58	31.46	32.98	34.24

Radiation	73 Tantalum	74 Tungsten	75 Rhenium	76 Osmium	77 Iridium	78 Platinum	79 Gold	80 Mercury
TI KA	735.6	753.3	796.3	824.4	871.0	934.3	905.5	958.3
TI KB	580.8	597.5	630.7	652.5	688.3	733.8	720.0	760.0
CR KA	454.7	470.4	495.5	512.4	539.6	571.6	568.0	597.9
MN KA	363.2	377.6	397.0	410.4	431.4	454.5	456.8	479.6
CR KB	355.0	369.1	388.0	401.1	421.6	443.9	446.7	468.9
FE KA	292.8	305.7	320.9	331.5	348.0	364.6	370.5	388.2
MN KB	282.3	294.9	309.5	319.7	335.6	351.2	357.6	374.5
CO KA	238.3	249.7	261.8	270.3	283.4	295.2	303.3	317.0
FE KB	226.7	237.9	249.3	257.3	269.7	280.6	289.0	301.9
NI KA	195.4	205.6	215.3	222.0	232.5	241.0	250.1	260.8
CO KB	183.9	193.7	202.7	209.0	218.8	226.4	235.7	245.7
CU KA	161.5	170.5	178.3	183.8	192.2	198.2	207.8	216.2
NI KB	150.4	159.0	166.2	171.2	179.0	184.2	193.8	201.5
ZN KA	134.4	142.4	148.7	153.1	160.0	164.2	173.7	180.4
CU KB	123.9	131.5	137.3	141.3	147.6	151.2	160.6	166.6
ZN KB	102.8	109.5	114.1	117.5	122.5	124.9	133.9	138.6
MO KA	89.51	95.76	98.74	100.2	103.4	108.6	111.3	114.7
MO KB	66.07	70.57	72.47	74.13	77.20	80.23	82.33	85.30
RH KA	61.39	65.54	67.27	68.91	71.90	74.56	76.53	79.38
PD KA	54.35	57.96	59.50	61.06	63.80	66.00	67.79	70.42
AG KA	48.25	51.40	52.78	54.24	56.75	58.58	60.21	62.63
RH KB	44.88	47.77	49.06	50.47	52.85	54.48	56.02	58.32
PD KB	39.68	42.18	43.33	44.64	46.82	48.15	49.54	51.65
AG KB	35.17	37.35	38.38	39.60	41.59	42.68	43.93	45.87

TABLE 2.1C (*continued*)

Mass Attenuation Coefficients (μ/ρ) in $cm^2\ g^{-1}$

Radiation	81 Thallium	82 Lead	83 Bismuth	86 Radon	90 Thorium	92 Uranium	94 Plutonium
TI KA	990.6	1035	1066	1174	1098	1084	959.7
TI KB	784.9	820.0	846.5	930.2	992.6	862.3	1023
CR KA	616.9	644.5	667.2	731.4	844.1	774.0	803.2
MN KA	494.4	516.5	536.1	586.4	678.0	672.0	731.4
CR KB	483.3	504.9	524.2	573.2	663.0	657.1	771.6
FE KA	399.8	417.7	434.5	474.3	549.3	545.2	637.6
MN KB	385.7	402.9	419.2	457.5	530.1	526.2	614.9
CO KA	326.3	340.8	355.3	387.1	449.0	446.3	519.6
FE KB	310.7	324.5	338.4	368.6	427.7	425.3	494.6
NI KA	268.3	280.2	292.7	318.3	369.8	368.1	426.7
CO KB	252.7	263.8	275.8	299.7	348.4	346.9	401.6
CU KA	222.2	232.1	242.9	263.7	306.8	305.7	352.9
NI KB	207.1	216.3	226.5	245.7	286.0	285.2	328.7
ZN KA	185.3	193.5	202.9	219.9	256.2	255.6	293.9
CU KB	171.1	178.6	187.5	203.0	236.6	236.2	271.2
ZN KB	142.3	148.5	156.2	168.8	197.0	196.9	225.2
MO KA	119.4	122.8	125.9	117.2	99.46	96.67	48.84
MO KB	88.25	90.55	93.50	100.7	73.34	72.63	78.99
RH KA	82.02	84.13	87.01	93.78	95.00	67.79	73.69
PD KA	72.68	74.50	77.23	83.28	97.20	84.24	65.72
AG KA	64.56	66.14	68.73	74.14	86.29	86.92	58.76
RH KB	60.08	61.52	64.02	69.08	80.26	81.11	76.36
PD KB	53.15	54.39	56.74	61.24	70.95	72.09	78.34
AG KB	47.15	48.22	50.41	54.44	62.88	64.24	69.75

2.1. References

[1] ALLING, W. R. and JOHNSON, W. R. Exact Calculation of *K*-Shell and *L*-Shell Photoeffect, *Phys. Rev.* **139**, A1050–A1062 (1965).

[2] ALLISON, J. W. γ-Radiation Absorption Coefficients of Various Materials Allowing for Bremsstrahlung and other Secondary Radiations, *Austral. J. Phys.* **14**, 443–468 (1961).

[3] AZÁROFF, L. V. Theory of Extended Fine Structure of X-Ray Absorption Edges, *Rev. Mod. Phys.* **35**, 1012–1022 (1963).

[4] BEARDEN, J. A. and BURR, A. F. Re-evaluation of X-Ray Atomic Energy Levels, *Rev. Mod. Phys.* **39**, 125–142 (1967). See also NSRDS-NBS 14 (1967).

[5] BERGER, R. T. The X- or γ-Ray Energy Absorption or Transfer Coefficient: Tabulations and Discussion, *Rad. Res.* **15**, 1–29 (1961).

[6] BRYSK, H. and ZERBY, C. D. Photoelectric Cross Sections in the keV Range, *Phys. Rev.* **171**, 292–298 (1968).

[7] CAUCHOIS, Y. *Les Spectres de Rayons X et la Structure Electronique de la Matière*, Gauthier-Villars, Paris (1948).

[8] CROMER, D. T. Compton Scattering Factors for Aspherical Free Atoms, *J. Chem. Phys.* **50**, 4857–4859 (1969).

[9] CROMER, D. T. and MANN, J. B. Compton Scattering Factors for Spherically Symmetric Free Atoms, *J. Chem. Phys.* **47**, 1892–1893 (1967).

[10] CROMER, D. T. and WABER, J. T. Scattering Factors Computed from Relativistic Dirac–Slater Wave Functions, *Acta Cryst.* **18**, 104–109 (1965).

[11] CURIEN, H. Compton Scattering of X-rays, Section 3.4.

[12] DAVISSON, C. M. Interaction of γ-Radiation with Matter, Ch. 1, and γ-Ray Attenuation Coefficients, Appendix 1 in *Alpha-, Beta-,* and *Gamma-Ray Spectroscopy*, Vol. 1, K. Siegbahn, Ed., North-Holland, Amsterdam (1965).

[13] DEL GRANDE, N. KERR and OLIVER, A. J. Magnitude of Iron X-Ray *K*-Absorption Fine Structure at 297°K, *Bull. Amer. Phys. Soc.* (Ser. 2), **16**, 545 (1971).

[14] DESLATTES, R. D. Estimates of X-ray Attenuation Coefficients for the Elements and Their Compounds, *Acta Cryst.* **A25**, 89–93 (1969).

[15] DOWE, R. M. Attenuation Cross Sections of Thallium at 122 keV, Dissertation, Univ. of Alabama (1965).

[16] EVANS, R. D. Compton Effect, pp. 218–298 in *Encyclopedia of Physics*, Vol. XXXIV, S. Flügge, Ed., Springer-Verlag, Berlin (1958).

[17] EVANS, R. D. X-Ray and γ-Ray Interactions, Ch. 3 in *Radiation Dosimetry*, Vol. I (Fundamentals), F. H. Attix and W. C. Roesch, Eds., Academic Press, New York (1968).

[18] FAESSLER, A. Röntgenspektrum und Bindungszustand, pp. 769–868 in *Landolt-Börnstein Zahlenwerte und Funktionen*, Vol. 1, Part 4, A. Eucken, Ed., Springer-Verlag, Berlin (1955).

[19] GRODSTEIN, G. W. X-Ray Attenuation Coefficients from 10 keV to 100 MeV, NBS Circ. 583 (1957).

[20] HAGSTRÖM, S., NORDLING, C., and SIEGBAHN, K. Tables of Electron Binding Energies and Kinetic Energy *versus* Magnetic Rigidity, App. 2 in *Alpha-, Beta-, and Gamma-Ray Spectroscopy*, Vol. I, K. Siegbahn, Ed., North-Holland, Amsterdam (1965).

[21] HALL, H. and SULLIVAN, E. C. *K*-Shell Photoeffect Cross Sections for the Fermi–Thomas Potential from 300 keV to 1·3 MeV, *Phys. Rev.* **152**, 4–9 (1966).

[22] HARTREE, D. R., KRONIG, R. DE L., and PETERSEN, H. A Theoretical Calculation of the Fine Structure for the *K* Absorption Band of Ge in $GeCl_4$, *Physica*, **1**, 895–924 (1934).

[23] HUBBELL, J. H. Photon Cross Sections, Attenuation Coefficients, and Energy Absorption Coefficients from 10 keV to 100 GeV, NSRDS-NBS 92 (1969).

[24] HULTBERG, S., NAGEL, B., and OLSSON, P. Numerical Calculation of *K*-Shell Photoeffect, *Ark. Fys.* **38**, 1–96 (1968).

[25] IBERS, J. A. Atomic Scattering Factors for X-rays (Corrected to November 1961). Vol. III, Sec. 3.3.1.

[26] ICRU (International Commission on Radiation Units and Measurements, TAYLOR, L. S., Chmn.): *Radiation Quantities and Units*, ICRU Rep. 11 (1968).

[27] KOCH, B., MACGILLAVRY, C. H., and MILLEDGE, H. J. X-ray Absorption, Vol. III, Sec. 3.2.1, and Calculated Absorption Coefficients of the Elements ($Z=1$ to 83), Vol. III, Sec. 3.2.2.

[28] KOSSEL, W. Zum Bau der Röntgenspektren, *Z. Phys.* **1**, 119–134 (1920); Über die Ausbildung der Röntgenserien mit wachsender Ordnungzahl, *Z. Phys.* **2**, 470–478 (1920).

[29] KRONIG, R. DE L. Zur Theorie der Feinstruktur in den Röntgenabsorptionsspektren, *Z. Phys.* **70**, 317–323 (1931).

[30] LIBERMAN, D., WABER, J. T., and CROMER, D. T. Self-Consistent-Field Dirac–Slater Wave Functions for Atoms and Ions. I. Comparison with Previous Calculations, *Phys. Rev.* **13**, A27–A34 (1965).

[31] LYTLE, F. W. *Determination of Interatomic Distances from X-Ray Absorption Fine Structure*, Boeing Scientific Research Laboratories (Seattle), Report D1-82-0524 (1966).

[32] MCGUIRE, E. J. Photo-Ionization Cross Sections of the Elements Helium to Xenon, *Phys. Rev.* **175**, 20–30 (1968).

[33] MCMASTER, W. H., DEL GRANDE, N. KERR, MALLETT, J. H., and HUBBELL, J. H. Compilation of X-Ray Cross Sections, Lawrence Radiation Laboratory (Livermore) Report UCRL-50174, Sec. I (1970); Sec. II, Rev. 1 (1969); Sec. III (1969); Sec. IV (1969).

[34] MOTZ, J. W., OLSEN, H. A., and KOCH, H. W. Pair Production by Photons, *Rev. Mod. Phys.* **41**, 581–739 (1969).

[35] MOTZ, J. W. and MISSONI, G. Compton Scattering by *K*-Shell Electrons, *Phys. Rev.* **124**, 1458–1468 (1961).

[36] PARRATT, L. G. X-Ray Resonance Absorption Lines in the Argon *K* Spectrum, *Phys. Rev.* **56**, 295–297 (1939).

[37] PARRATT, L. G. Electronic Band Structure of Solids by X-Ray Spectroscopy, *Rev. Mod. Phys.* **31**, 616–645 (1959).

[38] PARTHASARADHI, K., LAKSHMINARAYANAN, A. V., and JNANANANDA, S. Absolute Photoelectric Cross Sections of [145, 320, and 662 keV] γ-Rays [in Cu, Ag, Sn, Ta, Pt, and Pb], *Indian J. Pure Appl. Phys.* **2**, 290–292 (1964); **2**, 306 (1964); **3**, 223–224 (1965); **4**, 87–88 (1966); *Phys. Rev.* **142**, 9–11 (1966).

[39] PIRENNE, M. H. *The Diffraction of X-Rays and Electrons by Free Molecules*, Cambridge Univ. Press (1946).

[40] PRATT, R. H., LEVEE, R. D., PEXTON, R. L., and ARON, W. *K*-Shell Photoeffect Cross Sections from 200 keV to 2 MeV, *Phys. Rev.* **134**, A898–A915 (1964).

[41] RAKAVY, G. and RON, A. Atomic Photoeffect in the Range $E_\gamma = 1$–2000 keV, *Phys. Rev.* **159**, 50–56 (1967).

[42] SAMSON, J. A. R. The Measurement of the Photoionization Cross Sections of the Atomic Gases, in *Advances in Atomic and Molecular Physics*, Vol. 2, BATES, D. R., Ed., Academic Press, New York (1966), Table XXXII, p. 237, typographically corrected.

[43] SANDSTRÖM, A. E. Experimental Methods of X-Ray Spectroscopy: Ordinary Wavelengths, pp. 78–245 in *Encyclopedia of Physics*, Vol. XXX, Part 2, S. Flügge, Ed., Springer-Verlag, Berlin (1957).

[44] SCHMICKLEY, R. D. and PRATT, R. H. *K*-, *L*-, and *M*-Shell Atomic Photoeffect for Screened-Potential Models, *Phys. Rev.* **164**, 104–116 (1967).

[45] SELTZER, S. National Bureau of Standards, Washington D.C., hydrogen photoeffect calculations, private communication (1967).

[46] STENSTRÖM, W. Dissertation, Lund (1919). First published observation of absorption-edge fine structure, according to Sandström (Dissertation, Uppsala, 1935).

[47] STEPHENSON, S. T., KROGSTAD, R., and NELSON, W. The *K* X-Ray Absorption Structure of Cl_2 and HCl, *Phys. Rev.* **84**, 806–809 (1951).

[48] STORM, E. and ISRAEL, H. I. Photon Cross Sections from 0·001 to 100 MeV for Elements 1 through 100, Los Alamos Sci. Lab. Report LA-3753 (1967).

[49] THEISEN, R. and VOLLATH, D. Tables of X-Ray Mass Attenuation Coefficients, Verlag Stahleisen mbH., Düsseldorf (1967).

[50] TITUS, W. F. Total Photoelectric Cross Sections of Copper, Molybdenum, Silver, Tantalum, and Gold at 662 keV, *Phys. Rev.* **115**, 351–356 (1959).

[51] VEIGELE, W. J., TRACY, P. T., and HENRY, E. M. Compton Effect and Electron Binding, *Amer. J. Phys.* **34**, 1116–1121 (1966).

[52] ANDREWS, C. L. *Phys. Rev.* **54**, 994 (1938).

[53] ARGYLE, P. E., GRIFFITHS, G. M., and WARREN, J. B. *Canad. J. Phys.* **29**, 83 (1951).

[54] BACKHURST, I. *Phil. Mag.* **7**, 353 (1929).

[55] BAURMANN, E. and ULMER, K. *Z. Naturforsch.* **A12**, 670 (1957).

[56] BEARDEN, A. J. *J. Appl. Phys.* **37**, 1681 (1966).

[57] BECKMAN, O., AXELSSON, B., and BERGVALL, P. *Ark. Fys.* **15**, 567 (1959).

[58] BELL, P. R., RICHARDSON, J. E., and HEATH, R. L. Absorption of γ-Rays, in Oak Ridge National Laboratory report ORNL-1365 (Progress report for period ending June 20, 1952).

[59] BEZDENEZHNYKH, G. V., ZAPYSOV, A. L., ISRAILEV, I. M., and SAPRYKIN, V. N. *Opt. Spectrosc.* (USSR), **23**, 533 (1967).

[60] BIERMANN, H. *Ann. Phys.* **26**, 740 (1936).

[61] BUCKMAN, W. G. *The Determination of Low-Energy Mass Attenuation Coefficients of Argon (6–24 keV) and Carbon Dioxide (6–12 keV)*, M.S. Thesis, Vanderbilt University, Nashville, Tennessee (1962).

[62] CALLISEN, F. *Z. Phys.* **107**, 15 (1937).

[63] CARTER, R. W., ROHRER, R. H., CARLTON, W. H., and DYER, G. R. *Health Phys.* **13**, 593 (1967).

[64] CHIPMAN, D. R. and JENNINGS, L. D. *Phys. Rev.* **132**, 728 (1963).

[65] COLGATE, S. A. *Phys. Rev.* **87**, 592 (1952).

[66] COLVERT, W. W. *Phys. Rev.* **36**, 1619 (1930).

[67] COOKE, B. A., POUNDS, K. A., RUSSELL, P. C., and STEWARDSON, E. A. *Proc. Phys. Soc.* **79**, 883 (1962).

[68] COOKE, B. A. and STEWARDSON, E. A. *Brit. J. Appl. Phys.* **15**, 1315 (1964).

[69] COOPER, M. J. *Acta Cryst.* **18**, 813 (1965).

[70] CORK, J. M. *Phys. Rev.* **67**, 53 (1945).

[71] COWAN, C. L. *Phys. Rev.* **74**, 1841 (1948).

[72] CROWTHER, J. A. and ORTON, L. H. H. *Phil. Mag.* **10**, 329 (1930); **13**, 505 (1932).

[73] CUYKENDALL, T. R. *Phys. Rev.* **50**, 105 (1936).

[74] DALTON, J. L. Department of Energy, Mines and Resources, Canada, Experimental values, private communication (1968).

[75] DAVISSON, C. M. and EVANS, R. D. *Phys. Rev.* **81**, 404 (1951).

[76] DEL GRANDE, N. KERR, MALLETT, J. H., and OLIVER, A. J. Lawrence Radiation Laboratory, Livermore, California, Unpublished experimental results (1968).

[77] DEL GRANDE, N. KERR, STINNER, R. J., and OLIVER, A. J. Lawrence Radiation Laboratory, Livermore, California, Unpublished experimental results (1966–8).

[78] DERSHEM, E. and SCHEIN, M. *Phys. Rev.* **37**, 1238 (1931).

[79] DESLATTES, R. D. *An Experimental Study of X-ray Attenuation Coefficients, 8–30 keV*, AFOSR Report TN-58-784 (1958). See also Dissertation, Johns Hopkins Univ., Baltimore (1959).

[80] DEUTCH, B. I. and METZGER, F. R. *Phys. Rev.* **122**, 848 (1961).

[81] EHRENFRIED, C. E. and DODDS, D. E. *X-ray Mass Attenuation Coefficients in the 1·49 to 11·9 keV Range*, AFSWC Technical Note, AFSWC-TN-59-33 (1960).

[82] EKSTIG, B. *Ark. Fys.* **37**, 107 (1968).
[83] GANEEV, A. S. and IZRAILEV, I. M. *Sov. Phys. – Tech. Phys.* **5**, 1016 (1961).
[84] GLASER, H. *Phys. Rev.* **82**, 616 (1951).
[85] GROSSKURTH, K. *Ann. Phys.* **20**, 197 (1934).
[86] HANSEN, H. *Ann. Phys.* **35**, 524 (1939).
[87] HEINRICH, K. F. J. X-ray Absorption Uncertainty, in *The Electron Microprobe*, pp. 296–350. T. D. McKinley, K. F. J. Heinrich, and D. B. Wittry, Eds., Wiley, New York (1966).
[88] HENKE, B. L., ELGIN, R. L., LENT, R. E., and LEDINGHAM, R. B. *X-ray Absorption in the 2 to 200 Å Region*, Report number AFOSR 67–1254 (1967); also in *Norelco Rep.* **14**, 112 (1967).
[89] HON, P. K. and HEINRICH, K. F. J. National Bureau of Standards, Washington D.C., Unpublished experimental results, private communication (1968).
[90] HOPKINS, J. I. *J. Appl. Phys.* **30**, 185 (1959).
[91] HOWLAND, P. R. and KREGER, W. E. *Phys. Rev.* **95**, 407 (1954).
[92] HUBBELL, J. H. National Bureau of Standards, Washington D.C., unpublished experimental results (1967).
[93] HUGHES, G. D. and WOODHOUSE, J. B. X-ray Mass Absorption Coefficients, in *X-Ray Optics and Microanalysis*, pp. 202–209. R. Castaing, P. Deschamps, and J. Philibert, Eds., Hermann, Paris (1966); *J. Phys. D, Appl. Phys.* **1**, 695 (1968).
[94] JONES, M. T. *Phys. Rev.* **50**, 110 (1936).
[95] KNERR, R. P. and VONACH, H. *Z. Angew. Phys.* **22**, 507 (1967).
[96] LAKSHMINARAYANAN, A. V. and JNANANANDA, S. *Proc. Phys. Soc.* **77**, 593 (1961); *J. Sci. Ind. Res.* (India), **20B**, 1 (1961).
[97] LAUBERT, S. *Ann. Phys.* **40**, 553 (1941).
[98] LUKIRSKII, A. P. and ZIMKINA, T. M. *Bull. Acad. Sci.* (USSR), *Phys. Ser.* **27**, 808 (1963).
[99] MARTIN, L. H. and LANG, K. C. *Proc. Roy. Soc.* A**137**, 199 (1932).
[100] MATIN, P. *The Measurement of X-ray Mass Absorption Coefficients and Jump Ratios at Low Energies*, M.S. Thesis, Vanderbilt University, Nashville, Tennessee (1960).
[101] MCCRARY, J. H., PLASSMANN, E. H., PUCKETT, J. M., CONNER, A. L., and ZIMMERMANN, G. W. *Phys. Rev.* **153**, 307 (1967); private communication (1968).
[102] MÜLLER, I. *Ann. Phys.* **32**, 625 (1938).
[103] MURTY, R. C. *Proc. Phys. Soc.* **84**, 1032 (1964).
[104] NORDFORS, B. *Ark. Fys.* **19**, 259 (1961); NORDFORS, B. and NORELAND, E. *Ark. Fys.* **20**, 1 (1961); NORELAND, E. *Ark. Fys.* **23**, 273 (1962).
[105] OGIER, W. T., LUCAS, G. J., and PARK, R. J. *Appl. Phys. Lett.* **5**, 146 (1964).
[106] OLSON, A. R., DERSHEM, E., and STORCH, H. H. *Phys. Rev.* **21**, 30 (1923).
[107] PANZER, W. and PERZL, F. Institut für Strahlenschutz, München. Paper presented to: Premier Congrès Européen de Radioprotection, Menton, France (October 1968).
[108] PERKIN, J. L. and DOUGLAS, A. C. *Proc. Phys. Soc.* **92**, 618 (1967).
[109] QUIVY, R. *J. Phys. Radium*, **27**, 94 (1966).
[110] RAO, A., RAO, J., LAKSHMINARAYANAN, A. V., and JNANANANDA, S. *Indian J. Pure Appl. Phys.* **1**, 350 (1963).
[111] READ, J. *Proc. Roy. Soc.* A**152**, 402 (1935).
[112] READ, J. and LAURITSEN, C. C. *Phys. Rev.* **45**, 433 (1934).
[113] ROOF, R. B. JR. *Phys. Rev.* **1.3**, 820, 826 (1959).
[114] SCHNOPPER, H. W. *Phys. Rev.* **131**, 2558 (1963).
[115] SCHULZ, K. *Ann. Phys.* **27**, 1 (1936).
[116] SPENCER, R. G. *Phys. Rev.* **38**, 1932 (1931).
[117] SWEENEY, W. R., SEAL, R. T., and BIRKS, L. S. *Spectrochim. Acta*, **17**, 364 (1961).
[118] WIEDENBECK, M. *Phys. Rev.* **126**, 1009 (1962).
[119] WISE, P. R. *Low Energy X-Ray Mass Attenuation Coefficients for Radiation 850 to 3000 eV in Selected Elements with Z=6 to Z=18*, Report NP–12661 (1961).
[120] WOERNLE, B. *Ann. Phys.* **5**, 475 (1930).
[121] WREDE, W. *Ann. Phys.* **36**, 681 (1939).
[122] WUILLEUMIER, F. *J. Phys. Radium*, **26**, 776 (1965).
[123] WYARD, S. J. *Phys. Rev.* **87**, 165 (1952); *Proc. Phys. Soc.* **66A**, 382 (1953).
[124] BRAGG, W. H. and PEIRCE, S. E. *Phil. Mag.* **28**, 626–630 (1914).
[125] HEWLETT, C. W. *Phys. Rev.* **17**, 284–301 (1921).
[126] TAYLOR, E. G. *Phys. Rev.* **20**, 709–714 (1922).
[127] WINGARDH, K. A. *Z. Phys.* **8**, 363–376 (1922).
[128] TARRANT, G. T. P. *Proc. Roy. Soc.* A**128**, 345–359 (1930).
[129] MEITNER, L. and HUPFELD, H. H. *Z. Phys.* **67**, 147–168 (1931).
[130] KÜSTNER, H. *Z. Phys.* **77**, 52–59 (1932).
[131] ALLEN, S. J. M. *Handbook of Chemistry and Physics*, 18th ed., Chemical Rubber Co., Cleveland (1933), also subsequent editions. Only published version of certain of Allen's measured data.
[132] MESSNER, R. H. *Z. Phys.* **85**, 727–740 (1933).
[133] STEPHENSON, R. J. *Phys. Rev.* **43**, 527–533 (1933).
[134] HAHN, T. M. *Phys. Rev.* **46**, 149–153 (1934).
[135] KETELAAR, H., PICCARD, A., and STAHEL, E. *J. Phys. Radium*, **5**, 385–388 (1934).
[136] MAYNEORD, W. V. and ROBERTS, J. E. *Nature*, **136**, 793 (1935).
[137] JACOBSEN, J. C. *Z. Phys.* **103**, 747–755 (1936).
[138] MAYNEORD, W. V. and CIPRIANI, A. J. *Canad. J. Res.* **25A**, 303–314 (1947).
[139] ROSENBLUM, E. S., SCHRADER, E. F., and WARNER, R. M. JR. *Phys. Rev.* **88**, 612–167 (1952).
[140] SHIMIZU, S., HANAI, T., and OKAMOTO, S. *Phys. Rev.* **85**, 290–294 (1952).
[141] PAUL, R. S. *Phys. Rev.* **96**, 1563–1565 (1954).
[142] MAHMOUD, K. A. *Proceedings of the Third Arab Science Congress, Cairo*, pp. 726–740 (1957).
[143] TOMBOULIAN, D. H., BEDO, D. E., and NEUPERT, W. M. *J. Phys. Chem. Solids*, **3**, 282–302 (1957).
[144] WIEDENBECK, M. L. Unpublished gas data in TID-13923 (1961).
[145] BASHANDY, E. *Int. J. Appl. Rad. Isotopes*, **13**, 173–178 (1962).
[146] GATES, D. C., KENNEY, R. W., and SWANSON, W. P. *Phys. Rev.* **125**, 1310–1318 (1962); numerical data in: D. C. Gates, Thesis, Univ. of Calif., Berkeley (1960).

F

[147] KANEMORI, Y. Quoted by K. Tamaru and A. Tsuruo: *Nucl. Sci. Eng.* **28,** 144–145 (1967).

[148] MIDDLETON, R. M. and GAZZARA, C. P. *Acta Cryst.* **23,** 712–714 (1967).

[149] SCHMICKLEY, R. D. Private communication.

Added in proof:

[150] More recent values [STORM, E. and ISRAEL, H. I. Photon Cross Sections from 1 keV to 100 MeV for Elements $Z=1$ to $Z=100$, *Nucl. Data,* **7,** 565 (1970)] for hydrogen differ from those in Reference [33] by less than 0·5% in the energy range of Tables 2.1B and 2.1C.

[151] Recent measurements of the magnitude and extended energy range of fine-structure undulations were reported [DEL GRANDE, N. KERR and OLIVER, A. J. The Magnitude and Extended Energy Range of X-ray *K*-Absorption Fine Structure for Ti, Fe, Co, Ni, Cu, and Zn. *Proceedings of International Symposium on X-Ray Spectra and Electronic Structure of Matter.* A. Faessler, Editor, University of Munich (in the press); Lawrence Radiation Laboratory (Livermore) Report UCRL 73923, Rev. 1 (September, 1972)] for six metals, Ti–Zn. They found that the average behavior of the total attenuation coefficients had a steeper slope at energies approaching the *K*-edge from the high-energy side than was obtained previously for these metals in reference [33]. This would raise the center of the envelope described in Section 2.1.2 (footnote). A comparison of the new data with the previous values in reference [33] from which Tables 2.1A and 2.1B are derived is shown in Fig. 2.1.4(2) and discussed below to emphasize the uncertainties related to fine structure which are discussed in Section 2.1.4.

The measurements were taken at intervals $\lesssim 5$ eV from $\sim$20 eV to $\sim$1 keV above the *K*-edge, using a single-crystal spectrometer. Uncertainties were $\pm 2\%$ or less. A smooth average through the data was obtained by taking a least-squares fit to over 150 values of $\log(\mu/\rho)$ *versus* $\log E$, which was extended to the *K*-edge. The respective *K*-edge values for Ti, Fe, Co, Ni, Cu, and Zn were 6%, 10%, 3%, 8%, 8%, and 5% higher than the values in Reference [33]. At about 1 keV above the respective *K*-edges of these elements, differences were $\pm 2\%$ or less. The magnitudes of the undulations were $\pm 12\%$ or less from 40 eV to 200 eV (which is included in *Category D*) and $\pm 7\%$ or less from 200 eV to 1 keV (which is included in *Category C*) above the *K*-edge. The uncertainties discussed in Section 2.1.4 are thus shown to be sufficiently cautious for the examples illustrated in Fig. 2.1.4(2).